arXiv:chao-dyn/9506009v1 29 Jun 1995

Lyapunov spectral analysis of a nonequilibrium Ising-like transition

Corey S. O'Hern*, David A. Egolf†, and Henry S. Greenside‡

Department of Physics

Duke University

Durham, NC 27708-0305

(June 17, 1995)

Abstract

By simulating a nonequilibrium coupled map lattice that undergoes an Ising-like phase transition, we show that the Lyapunov spectrum and related dynamical quantities such as the dimension correlation length ξ_δ are insensitive to the onset of long-range ferromagnetic order. As a function of lattice coupling constant g and for certain lattice maps, the Lyapunov dimension density and other dynamical order parameters go through a minimum. The occurrence of this minimum as a function of g depends on the number of nearest neighbors of a lattice point but not on the lattice symmetry, on the lattice dimensionality or on the position of the Ising-like transition. In one-space dimension, the spatial correlation length associated with magnitude fluctuations and the length ξ_δ are approximately equal, with both varying linearly with the radius of the lattice coupling.

47.27.Cn, 05.45.+b, 05.70.Ln, 82.40.Bj

Typeset using REVTEX

I. INTRODUCTION

Laboratory experiments [1] and numerical simulations [2] can now systematically explore sustained homogeneous nonequilibrium systems of quite large aspect ratios ($\Gamma \lesssim 1000$) which possibly approximate a thermodynamic limit of infinite system size. These advances raise the theoretical question of identifying order parameters for analyzing and classifying spatiotemporal chaotic states so that a quantitative comparison can be made between theory and experiment [3]. The most appropriate order parameter for a given nonequilibrium system is presently not well understood although numerous possibilities have been studied. Some order parameters, such as spatial correlation lengths obtained from exponentially decaying correlation functions, emphasize the average spatial disorder and have been widely used in condensed matter physics [4]. Others such as the metric entropy and the Lyapunov fractal dimension [5] are familiar from nonlinear dynamics and emphasize the average temporal disorder or dynamical complexity arising from the geometric structure of an attractor in phase space.

We would then like to know whether these different kinds of order parameters are related and whether there is a need for new order parameters. As an example, does knowledge of an easily measured correlation length give information about the fractal dimension, which is difficult to estimate from experimental time series [6]? That a relation between spatial disorder and dynamical complexity may exist is suggested by the prominence in many nonequilibrium states of defects [7] whose dynamics often determine the average spatial disorder [8]. Examples of defects are amplitude holes in one-dimensional complex Ginzburg-Landau equation (abbreviated below as CGLE) [9–12], domain walls and droplets of opposite spin in coupled map lattices (CMLs) with an Ising-like transition [13,14], vortices in the two-dimensional CGLE [8], and spirals and centers in the recently discovered spiral-defect chaos state in thermal convection [15]. The nucleation, motion, and annihilation of defects are important features of the chaotic dynamics and so dynamical quantities such as the fractal dimension may be related to their spatial statistics [16–18]. Complicating this simple picture is the

fact that not all fluctuations are associated with defect motion, e.g., phase fluctuations in the CGLE [11,19]. The fractal dimension may then be larger than that suggested by defect statistics.

In recent work [17,12,19], Egolf and Greenside have explored the relation between temporal and spatial disorder for the CGLE on a large periodic interval [11]. Observing that sufficiently large chaotic systems become extensive so that a fractal dimension D grows linearly with volume size $V \propto L^d$ (where L is the system size and d is the spatial dimensionality) [7,20–22,17,23,24], they calculated the dimension correlation length ξ_δ which is defined [7] in terms of the intensive dimension density

$$\delta = \lim_{L\to\infty} D/V, \tag{1}$$

by the equation

$$\xi_\delta = \delta^{-1/d}. \tag{2}$$

The length ξ_δ can be interpreted crudely as a characteristic size of dynamically independent subsystems or a characteristic range of chaotic fluctuations. Near a transition from phase- to defect-turbulent states [11,25], Egolf and Greenside found that the length ξ_δ was approximately equal to, and had the same parametric dependence as, the spatial correlation length given by the magnitude fluctuations of the Ginzburg-Landau field [12]. Over the same parameter range, the correlation length ξ_ϕ arising from phase fluctuations (and also of the Ginzburg-Landau field itself) was found to increase to quite large values, suggesting that the chaos fluctuations measured by ξ_δ were short-ranged and decoupled from the phase.

In this paper, the one-dimensional investigations of Egolf and Greenside [17,12] are extended by examining similar questions of how spatial disorder and dynamical complexity are related for spatial dimensionality $d = 2$ and $d = 3$. We study a class of dissipative coupled map lattices [14] that undergoes an Ising-like ferromagnetic-ordering transition as a lattice coupling constant g (defined below in Eq. (4)) is increased through a range of finite positive values, corresponding to a transition from a high-temperature paramagnetic phase

to a low-temperature ferromagnetic phase. Instead of the point-like space-time defects of the one-dimensional CGLE [12], long-lived defects occur in the form of domain walls and droplets involving regions of opposite sign. At a critical transition point $g = g_c$, the usual two-point correlation length ξ_2 diverges to infinity while the magnetization (the average of the signs of all lattice variables) bifurcates from a zero to nonzero value. The main attraction of the Miller-Huse model [14] is that a transition with a diverging correlation length occurs from one chaotic state to another. This permits a careful comparison of different length scales near the transition point.

By calculating the Lyapunov spectrum and related dynamical quantities such as the dimension correlation length ξ_δ, we show that correlations in chaotic fluctuations near the ordering transition have a short range and are decoupled from the diverging long-range order measured by the length ξ_2. As was the case for the 1d periodic CGLE [12], the length ξ_δ and the correlation length $\xi_2^{\rm mag}$ arising from magnitude fluctuations of the CML variables both turn out to be short—here about one lattice spacing—but a quantitative relation can not be determined since these lengths do not vary substantially with parameters. In one-space dimension, a more substantial variation in these quantities is obtained by increasing the radius r of the coupling from nearest to rth-nearest lattice neighbors. With increasing radius r, the lengths ξ_δ and $\xi_2^{\rm mag}$ then increase approximately linearly and with slopes related by a factor of order one. This suggests that the two lengths may be related and that r is important in determining the length scale of dynamical fluctuations.

Several dynamical quantities such as the largest Lyapunov exponent λ_1, the metric entropy density $h = \lim_{L\to\infty} H/V$, and the Lyapunov fractal dimension density δ attain minimum values near—but distinctly not at—the critical transition point $g = g_c$. At first glance, minima in quantities such as h or δ seem counterintuitive since the onset of ferromagnetic ordering should correspond to increased correlations, i.e., decreased dynamical complexity and a decreased dimension density or entropy density. Such a monotonic decrease in the metric entropy is, in fact, observed for a non-dissipative equilibrium CML that undergoes an Ising-like transition [13]. But because the dimension correlation length ξ_δ is quite short in the

Miller-Huse model, we argue below that dynamical quantities are only sensitive to nearest neighbor dynamics. As the coupling constant g increases, the discrete Laplacian eventually becomes antidiffusive, magnifying rather than reducing short-wavelength structure, and the dimension density and entropy density start to increase.

The role of coupling lattice neighbors is demonstrated with calculations on periodic 2d hexagonal and 3d cubic lattices. For these cases, ξ_δ is again about one lattice spacing in size and the extrema in dynamical quantities occur at a value $g \approx 1/(n+1)$ determined by the number n of nearest neighbors ($n = 4$ for the square lattice, $n = 6$ for the hexagonal and cubic lattices). The positions of the extrema do not coincide with the bifurcation of the magnetization and do not seem to depend on the lattice symmetry and dimensionality. The origin of these minima remains to be explained.

These results, together with previous work on the 1d CGLE and with some unpublished work on CMLs with algebraic decay of spatial correlations [24], suggest that the dimension correlation length will typically be short so that chaotic fluctuations are decoupled from long-range spatial order as measured by correlation functions. This leads to the qualitative conclusion that defects, although a striking visual feature of spatiotemporal chaos, are not the source of complexity that leads to large fractal dimensions and to small dimension correlation lengths. The physical meaning and utility of the length ξ_δ remains to be understood and further studies on different kinds of systems will be useful.

The rest of this paper is organized as follows. In Section II, we define the coupled map lattice and discuss some details of how its Lyapunov spectrum is calculated using a CM-5 parallel computer [26]. In Section III, we discuss various results of our simulations, especially the dependence of order parameters on the lattice coupling constant and on the symmetry and dimensionality of the lattice. Finally, in Section IV, we summarize our results and relate them to other recent research.

II. METHODS

In this section, we define the mathematical models used in our simulations and discuss some details about how the Lyapunov spectrum and spatial correlation lengths were calculated numerically. Since a CM-5 parallel computer played an important role in our being able to explore large space-time regions for many parameter values, we also discuss some details of how the algorithms were adapted for parallel computation.

A. Models

As easily simulated models of spatiotemporal chaos, we consider homogeneous coupled map lattices (CMLs) in which the same chaotic map $\phi(y)$ is associated with each point of a finite periodic lattice and for which nearest neighbor maps are coupled linearly by diffusion. CMLs have a significant advantage over partial differential equations of being analytically amenable [27] and easier to simulate on a computer. CMLs have the drawback that their solutions can not generally be related quantitatively to experiment and they may not have universal critical properties near transitions [28].

We study CMLs suggested by recent work of Miller and Huse [14], who analyzed the long-wavelength properties of a two-dimensional CML that orders ferromagnetically, in analogy to the equilibrium Ising model [29]. Following these authors, we use a lattice map $\phi(y) = -\phi(-y)$ with odd symmetry so that domains of opposite "spin" or sign arise. The odd symmetry is a necessary but not sufficient condition [30] for obtaining an Ising-like transition in which the magnetization (defined below in Eq. (8)) bifurcates to a nonzero value as a coupling constant g is varied. Following Miller and Huse, we choose $\phi(y)$ to be a piecewise-linear map with slope of constant magnitude greater than one, for which only chaotic states of constant measure exist in the absence of lattice coupling.

If y_i^t denotes the variable at spatial site i at integer time t (with $t = 0, 1, \cdots$), then the rule for updating each lattice variable to time $t + 1$ is given by [14]:

$$y_i^{t+1} = \phi(y_i^t) + g \sum_{j(i)} \left(\phi(y_j^t) - \phi(y_i^t) \right), \tag{3}$$

where the parameter g is the spatial coupling constant. The sum goes over indices $j(i)$ that denote nearest neighbors sites of site i, e.g., the four nearest neighbors on a square two-dimensional lattice or the six nearest neighbors in a 2d hexagonal lattice or 3d cubic lattice. For most of our calculations, we used the same local map as in Ref. [14]:

$$\phi(y) = \begin{cases} -2 - 3y & \text{for} \quad -1 \leq y \leq -1/3, \\ 3y & \text{for} \quad -1/3 \leq y \leq 1/3, \\ 2 - 3y & \text{for} \quad 1/3 \leq y \leq 1, \end{cases} \tag{4}$$

with a slope of constant magnitude equal to 3. To understand the competition between local chaos and diffusion (which decrease and increase spatial correlations respectively), we also used a more weakly chaotic map with a slope of smaller constant magnitude equal to 1.1:

$$\phi(y) = \begin{cases} -1.1x - 1.0 & \text{for } x \leq 0, \\ -1.1x + 1.0 & \text{for } x > 0. \end{cases} \tag{5}$$

Once a local map $\phi(y)$ has been chosen, a numerical simulation is specified by the dimensionality of the lattice d, the symmetry of the lattice (e.g., square, hexagonal, or cubic), the size of the lattice L (number of sites along an edge), the coupling constant g, the initial condition y_i^0, and the total integration time T. In this paper, we used an integer lattice in 1d, square and hexagonal lattices in 2d and a cubic lattice in 3d. Initial conditions consisted of assigning a random uniformly-distributed number in the interval $[-0.1, 0.1]$ to each site; results were not dependent on the choice of initial conditions provided the integration time was sufficiently long. Typical integration times were $T = 50,000$ iterations for calculations of Lyapunov exponents and $T = 150,000$ iterations for calculations of correlation functions. We made a few runs with longer integration times of $T = 60,000$ and $T = 500,000$ to check the convergence of the Lyapunov exponents and the correlation functions, respectively. Different lattice sizes were used depending on which order parameters were being studied, typically $L \leq 32$ for calculating Lyapunov exponents (which are quite costly to

compute) and $L \leq 1024$ for estimating correlation lengths. Many runs were repeated using several lattice sizes to verify the absence of significant finite-size effects.

For calculations of statistical averages such as the magnetization and correlation functions, the statistics could often be improved substantially by averaging the results of an ensemble of N runs each of duration T, with each run differing only in the choice of initial conditions. Calculations indicate that this ensemble average is ergodically equivalent to a single integration of duration NT [19,31]. For most of the results reported below, we used an ensemble average over $N = 64$ runs which could be executed simultaneously and in parallel on the vector units of a 16-node partition of a CM-5 computer.

B. Lyapunov Exponents and Associated Dynamical Quantities

Some dynamical order parameters can be constructed by combining in different ways the Lyapunov exponents λ_i associated with a given attractor [5]. For the CML given by Eq. (3) with a total of $N = L^d$ lattice sites, there are N real-valued Lyapunov exponents λ_i (labeled in decreasing order $\lambda_1 \geq \lambda_2 \geq \cdots \geq \lambda_N$) that characterize the long-time average-rate-of-separation of nearby orbits in phase space. From the λ_i, we can calculate a Lyapunov dimension D given by the Kaplan-Yorke formula [5]:

$$D = K + \frac{1}{|\lambda_{K+1}|} \sum_{i=1}^{K} \lambda_i, \tag{6}$$

and calculate an entropy defined by the sum of the positive exponents [5]:

$$H = \sum_{\lambda_i > 0} \lambda_i. \tag{7}$$

The number K in Eq. (6) is the largest integer such that the sum $\sum_{i=1}^{K} \lambda_i$ of the first K exponents is nonnegative; this sum is positive for $K = 1$ if an orbit is chaotic ($\lambda_1 > 0$) and is negative for $K = N$ if the dynamics is dissipative and so the sum typically crosses zero at an intermediate index $K \approx D$ for a chaotic dissipative system.

The exponents λ_i were calculated numerically by a now-standard numerical method [32], in which $K \leq N$ linearizations of the equations of motion, Eq. (3), are evolved in time. This

allows one to follow K Lyapunov vectors in a tangent space from which local stretching information and the Lyapunov exponents can be extracted. Together with a particular nonlinear orbit defined by the equations of motion, a total of $K+1$ CMLs was evolved to calculate K Lyapunov exponents.

Repeated orthonormalizations of Lyapunov vectors at time intervals T_n are needed to prevent floating-point overflow from the exponentially growing values and to prevent inaccuracies arising from the loss of linear independence as they fold up along the direction of the fasting growing exponent [32]. For the maps Eqs. (4) and (5), we found empirically that values $T_n \lesssim 30$ gave reasonable results for all lattices studied with the largest value of T_n depending on the parameters g and L. Smaller renormalization times did not change the values of the Lyapunov spectrum (although the code was more costly to run) while larger values led to serious errors due to linear dependence of the Lyapunov vectors.

The orthonormalizations of tangent vectors consumed most of the computing time on a Thinking Machines CM-5 parallel computer. The orthonormalizations require substantial communication between different processors since each processor evolves independently only a few of the K linearized equations in its own local memory; this communication decreases the efficiency of the code.

Although the communication inherent in the orthonormalization procedure could not be avoided, in all other portions of the code communication between nodes was eliminated by iterating redundantly an identical copy of the nonlinear CML Eq. (3) with identical initial conditions on each processor. In this way, information about the underlying orbit (needed when iterating the linearized CMLs) did not have to be communicated from one processor to all others at each time step.

By monitoring the Lyapunov exponents and the Lyapunov dimension as a function of time t, we found empirically that an integration time $T \gtrsim 50,000$ time steps gave an acceptable relative accuracy of better than one percent for calculating the dimension D and entropy H for all lattices studied ($L \leq 32$). Fig. 1 shows how the dimension D converges over time for lattice size $L = 16$ and for $g = 0.202$. The dimension curve is noisy with fluctuations

that diminish slowly over time (the λ_i, not shown, have substantially noiser time series). Goldhirsch et al [33] have argued that the amplitude of the exponent fluctuations should decay as $1/T$ where T is the total integration time and so one could fit and extrapolate to get a better estimate [22]. Extrapolation was not needed in plots like Fig. 1 which already give an adequate relative accuracy of better than one percent.

By repeating plots such as Fig. 1 for different system sizes L with all other parameters held fixed, we found extensive scaling of the dimension D with the volume of the system $N = L^2$ for a wide range of parameter values g, an example of which is given in Fig. 2. Fig. 2(a) shows that the dimension D increases linearly and extensively with N beyond a system size of about $L = 9$. The Lyapunov dimension density δ could then be obtained from the slope of a least-squares fitted line in the extensive region. The intercept of a least-squares-fitted line through the four right-most points was 0.007 which is quite small (and is also approximately zero for extensively chaotic solutions of the 1d CGLE [19]). There is then the possibility that a single dimension calculation for a sufficiently large system may suffice to estimate its dimension density. By comparing the dimension per volume D/L^2 with the dimension density δ, Fig. 2(b) shows how the extensive regime is approached rapidly and achieved for fairly small system sizes $L \geq 9$.

We finish this subsection with two comments about the meaning of the Lyapunov dimension D and about why we chose to calculate D from Lyapunov vectors rather than from time series measurements. The reader should recall that there is an infinity of fractal dimensions D_q (often called the Renyi dimensions) associated with a strange attractor with the parameter q varying over the real numbers [5]. Since each dimension D_q will be extensive for a homogeneous extensively chaotic system, the particular values only reflect the system size and are not interesting themselves. Instead, one should define a continuum of corresponding intensive dimension densities $\delta_q = \lim_{L\to\infty} D_q/V$ to provide a partial characterization of such systems.

For large fractal dimensions ($D \gtrsim 5$), present computers and algorithms only allow the calculation of the Lyapunov fractal dimension Eq. (6) and its corresponding density. The

Lyapunov dimension is conjectured to be the same as the Renyi dimension with $q = 1$ (i.e., the information dimension D_1 [5]) and it is not known to what extent the corresponding density δ_1 characterizes the unknown function of densities δ_q, e.g., whether it is close to the mean value of the δ_q. There are one-dimensional maps for which the ratio of D_1 to D_2 (the two most commonly calculated fractal dimensions) can be arbitrarily large [35], and so the variation of the function δ_q around its mean value can be large. A perhaps even more important question is whether the different dimension densities δ_q each have a similar dependence on model parameters, e.g., all increasing or decreasing together. Until this issue is resolved, the dimension density δ_1 and the corresponding length $\xi_\delta = \delta_1^{-1/d}$ need to be interpreted with caution.

The dynamical quantities D and H are calculated in terms of the Lyapunov spectrum λ_i, and not in terms of time series y_i^t at a given lattice site i, because of the impractical computational demands of time series algorithms [36]. While the computational complexity of the method based on the Lyapunov spectrum scales algebraically with system volume V or dimension D [37], it is well known that the computational complexity of classical time series algorithms such as that proposed by Procaccia and Grassberger grows *exponentially* with D, imposing severe restrictions on the largest dimension that can be estimated from experimental data. Although it remains controversial what is the practical upper bound for clean time series of less than a million points (there are claims from 6 to 20 [6]), existing time series methods can not treat extensively chaotic systems whose fractal dimensions may be in the hundreds (see Fig. 2).

C. Magnetization and Correlation Lengths

In addition to the dynamical quantities described in the previous section, we quantify the evolution of the CMLs by a "magnetization" M and by length scales measured from two-point and mutual information correlation functions. We describe these briefly to indicate the method and errors involved.

Following Miller and Huse [14], the average magnetization M of the CML is defined by a space-time and ensemble average of the signs ± 1 of the lattice values y_i^t,

$$M = \langle \mathrm{sign}(y_i^t) \rangle \equiv \frac{1}{NTp} \sum_{i,t,p} \mathrm{sign}(y_i^t(p)), \tag{8}$$

where the index p labels a particular CML running on processor p. An average over 64 independent CMLs running on a 16-node partition of a CM-5 was typically used. For the local maps Eq. (4) and Eq. (5), M undergoes a pitchfork bifurcation from a zero to finite value as the lattice coupling g is increased from small values. The critical value g_c at which M bifurcates to a nonzero value is unchanged if the values of the site variables y_i^t are used instead of their signs in Eq. (8). The bifurcation of M to a nonzero value defines the onset of ferromagnetic order at $g = g_c$ [14] as illustrated in Fig. 3.

To characterize the average spatial disorder, we examined two of many possible definitions of spatial correlation lengths, one from an exponentially decaying two-point correlation function, another from an exponentially decaying mutual information function [38]. (Some other correlation lengths are discussed on pages 945-947 of Ref. [7].) The two-point correlation function was defined in the usual way:

$$C_2(|\mathbf{X}_i - \mathbf{X}_{i'}|) = \left\langle (y_i^t - \langle y \rangle)\,(y_{i'}^t - \langle y \rangle) \right\rangle, \tag{9}$$

where $\mathbf{X}_i$ denotes the position of lattice point i and where the brackets $\langle \cdot \rangle$ denote the averaging process of Eq. (8). Given the periodicity of the lattice and the availability of efficient parallel Fast Fourier Transforms (FFTs) on the CM-5, we calculated Eq. (9) via the Wiener-Khintchin theorem [39], first obtaining the time-averaged magnitude squared of the Fourier coefficients, from which Eq. (9) was obtained by an inverse FFT. In most cases, there was a substantial region of exponential decay from which the two-point correlation length ξ_2 was obtained by a least-squares fit of the form $a \exp(-x/\xi_2)$; a representative plot is given in Fig. 4. The correlation functions and corresponding values of ξ_2 do not change if Eq. (9) is defined in terms of the sign of the variables, $\mathrm{sign}(y_i^t)$.

The two-point correlation functions decay more rapidly as shown in Fig. 5 if the signs of the field values y_i^t in Eq. (9) are replaced by their magnitudes $|y_i^t|$. The correlation length ξ_2^{mag}

obtained from the initial rapid exponential decay is approximately one lattice spacing and changes little when the coupling constant g is varied over a large range, including near the bifurcation point $g = g_c$. For dimensionality $d = 1$, we show below that this short length scale $\xi_2^{\rm mag}$ is related to the dimension correlation length ξ_δ and that both vary linearly with the radius r of neighboring lattice sites that are coupled together spatially.

As a possible alternative for characterizing the spatial disorder of a nonlinear system, we also calculated a correlation length ξ_I based on the exponential decay of the mutual information function $I(\triangle \mathbf{X})$ [38] of the variables y_i^t. Fig. 6 shows the exponential decay of a mutual information function $I(\triangle \mathbf{X})$ for two-dimensional square lattice of size $L = 256$ and for the parameter $g = 0.204$. Again if the magnitudes of the field variables are used when calculating $I(\triangle \mathbf{X})$, the exponential decay is much more rapid, with $\xi_I^{\rm mag}$ being approximately one lattice spacing for a wide range in g.

Although there is not yet a compelling theoretical reason to prefer ξ_I over other correlation lengths such as ξ_2 [7], the former has the distinction of depending nonlinearly on the dynamics and so may depend on details that are missed by ξ_2. For this reason, an increasing number of scientists have reported correlation lengths in terms of ξ_I [40,23,41]. As shown in Fig. 7 for the two-dimensional Miller-Huse CML on a square lattice, the length scales ξ_2 and ξ_I are linearly related over a substantial dynamical range near the ferromagnetic transition. At least for the present models, these lengths are equivalent measures of spatial disorder and we report values only for ξ_2 below.

III. RESULTS AND DISCUSSION

In this section, we discuss our calculations of the Lyapunov spectrum and of correlation lengths. Our goal is to explore how spatial disorder (as characterized by the two-point correlation length or by the mutual information correlation length) is related to dynamical complexity (as measured by the intensive dimension density and by the dimension correlation length Eq. (2)) and to investigate how these order parameters vary near the nonequilibrium

transition point $g = g_c$ at which the magnetization bifurcates to nonzero values (Fig. 3).

Results for the 2d square lattice are given first, followed by results for lattices with different symmetries and dimensionalities. We do not address issues related to critical exponents of these different models which have been discussed by Miller and Huse [14] and more recently by Marcq and Chaté [28]. Related interesting results on similar CMLs have also recently been reported by Boldrighini et al [30].

A. Results for Two-Dimensional Square Lattices

For the two-dimensional periodic square lattice with map Eq. (4), Fig. 3 shows that there is a bifurcation at $g_c \simeq 0.205$. This bifurcation corresponds to the onset of long-range order of the lattice variables y_i^t as demonstrated by the divergence of the two-point correlation length ξ_2 as g approaches g_c (Fig. 8(a)). Over this same parameter range, the dimension correlation length ξ_δ varies smoothly (Fig. 8(b)), deviating by less than four percent from a value of one lattice spacing and attaining a maximum value close to where the correlation length diverges. The Lyapunov spectrum of exponents also varies smoothly from one side of the transition to the other as shown in Fig. 9. We conclude that chaotic fluctuations have a short range, are decoupled from the onset of long-range order measured by ξ_2, and that the spectrum of exponents is at most weakly dependent on the onset of long-range spatial order.

To understand further how various dynamical quantities change near the transition point, we have plotted in Fig. 10 the variation of the Lyapunov fractal dimension density δ, of the metric entropy density h, and of the largest Lyapunov exponent λ_1 across the ferromagnetic transition for a lattice of size $L = 16$, which is already extensively chaotic according to Fig. 2. As was the case for the length ξ_δ in Fig. 8(b), these quantities change by only a small amount through the transition (at most by 20%) and all go through a minimum close to, but distinct from, the ferromagnetic transition at $g_c \approx 0.205$. This result was surprising to us since one consequence of coupling neighboring maps more strongly (increasing the parameter g) would

intuitively be to increase correlations between their dynamics, which should decrease both δ and h. Fig. 10(a) indicates that roughly one quarter of the maximum number of degrees of freedom disappear when the lattice attains its minimum dimension density of $\delta \approx 0.746$. (An upper bound of $\delta = 1$ is set by the integer lattice spacing.)

It is not clear why the fractal dimension density and other dynamical quantities have extrema near $g = 0.20$. For an equilibrium non-dissipative CML of Ising dynamics on a two-dimensional square lattice, Sakaguchi [13] did not find a local minimum in the entropy H but instead found a monotonic decrease consistent with the analytical solution of the spin-1/2 Ising model on a square lattice [29]. One explanation for the extrema may be that the dissipative linear coupling in Eq. (3) becomes antidiffusive for $g \geq 1/5$, enhancing rather than damping short-wavelength fluctuations and so decorrelating nearby lattice variables.

The issue is somewhat more subtle than this because the existence of the minimum depends also on details of the local map $\phi(y)$ in Eq. (3). For the less chaotic lattice map Eq. (5) with slope of constant magnitude 1.1, an Ising-like transition still occurs as shown by the bifurcation of the magnetization near $g_c \approx 0.168$ in Fig. 11. Fig. 12 now shows that the Lyapunov dimension density δ and entropy density h decrease monotonically as the parameter g is increased, with the largest exponent λ_1 remaining constant.

B. Results for Other Lattices

Figures 3, 8(a), and 10 suggest that the extrema of dynamical quantities may be related to the ferromagnetic transition. On the other hand, the short dimension correlation length in Fig. 8(b) contradicts this by implying that chaotic fluctuations occur over a length scale that is short compared to the ferromagnetic ordering. To understand this further, we have explored CMLs of different symmetry and dimensionality and found that the near-proximity of the extrema with the transition is a coincidence for the two-dimensional lattice with square symmetry. More generally, the positions of extrema seem to be determined simply by the number of nearest neighbors n, and not by the symmetry or dimensionality of the CML or

by the position of the magnetization bifurcation point.

Fig. 13 summarizes calculations for a two-dimensional periodic hexagonal lattice by plotting the dependence of magnetization M and of dimension correlation length ξ_δ on the coupling constant g. The magnetization bifurcates to a nonzero value at $g_c \approx 0.120$ which is a smaller value than that for the square lattice since the larger number of nearest neighbors (six versus four) increases the effective strength of the diffusive coupling. The relative difference between the transition at $g = g_c$ and the positions of the extrema in ξ_δ and in related dynamical quantities is substantially larger than was the case for the 2d square lattice. For the hexagonal lattice, extrema in quantities like the length ξ_δ occur at a value close to $g = 1/(n+1) \approx 0.143$ where $n = 6$ is the number of nearest neighbors.

A similar result is found for the same CML on a 3d cubic lattice, as shown in Fig. 14. The transition at $g \approx 0.11$ occurs at a value close to but smaller than the value on the hexagonal lattice. Extrema in the dynamical quantities like ξ_δ again occur at a value close to $1/(n+1)$ with $n = 6$.

That the positions of the extrema of dynamical quantities is dependent primarily on the number of nearest neighbors is a consequence of the nearest-neighbor diffusive coupling in Eq. (3) and of the fact that, for the local map Eq. (4), the chaos is sufficiently strong to make the dimension correlation length ξ_δ quite small, about one lattice length. That the positions of the extrema seem to be given quantitatively by the specific formula $g = 1/(n+1)$ is more delicate to understand but may be related to the fact that the discrete Laplacian operator changes from diffusive to antidiffusive behavior at this value. The value $g = 1/(n+1)$ is the value for which the weight of each of the neighbors is equal to the weight of the central lattice site to be updated.

For all CMLs that we studied, the dimension correlation length ξ_δ was about one lattice spacing in size and this was also the "radius" of the diffusive coupling in Eq. (3). This suggests that the length ξ_δ may be determined by the spatial extent of the diffusive coupling, becoming larger as more sites are coupled to a given site. This conjecture was tested in one-space dimension by coupling together, with equal weight g, all lattice variables within a

radius r of a given site i:

$$y_i^{t+1} = \phi(y_i^t) + g \sum_{j=i-r}^{i+r} \left(\phi(y_j^t) - \phi(y_i^t) \right). \tag{10}$$

For this one-dimensional periodic CML with the lattice map Eq. (4), the dynamics varies in a complicated way with radius r. For most initial conditions, chaos was found for smaller radii ($r < 6$). For larger radii $r \geq 6$, the transients lasted much longer and the asymptotic dynamics was periodic. As an example, for $r = 10$ the dimension as a function of time initially reached a value $D = 50$ even after 5000 transient iterations were skipped; however, the dimension then decreased steadily to zero over the next 30,000 iterations. We believe that this asymptotic periodic behavior is a finite-size effect. For a sufficiently large system size L, with the crossover length increasing with the radius r, the asymptotic state should be chaotic.

For dimensionality $d = 1$, the dimension correlation length ξ_δ varies more strongly with increasing radius r than with coupling constant g, which allows several different length scales to be compared. Fig. 15 shows that the two-point correlation length $\xi_2^{\rm mag}$ obtained using the magnitudes $|y_i^t|$ of the field values has approximately the same linear dependence on the coupling radius r as the dimension correlation length ξ_δ. In addition, these two length scales are the same order of magnitude. The two-point correlation length ξ_2 obtained using the actual field values is larger than ξ_δ and does not have the same simple linear dependence on r. The situation is then similar to results found for spatiotemporal chaotic solutions of the 1d periodic CGLE [12] in that the spatial correlation length of fluctuations in the magnitude of a field provides a way of estimating the length ξ_δ.

IV. CONCLUSIONS

In this paper, we have extended recent calculations [17,12,19] concerning the relation between spatial disorder and dynamical complexity of a sustained homogeneous nonequilibrium system from dimensionality $d = 1$ to dimensionalities $d = 2$ and $d = 3$. This

was accomplished by choosing a coupled map lattice, Eq. (3), that underwent an Ising-like transition with diverging two-point correlation length as a parameter g was varied [14]. By comparing various length scales such as the two-point correlation length ξ_2, the dimension correlation length ξ_δ, and the two-point correlation length of magnitude fluctuations $\xi_2^{\rm mag}$ near the transition point, we were able to show that the lengths ξ_δ and $\xi_2^{\rm mag}$ were short, of order one lattice spacing, even as the length ξ_2 diverged to infinity. In agreement with previous work [12], the chaotic fluctuations are decoupled from the average long-range spatial order. The correlation length of magnitude fluctuations seems to provide an effective way to estimate the size of the length ξ_δ.

Our calculations of the Lyapunov spectrum and related quantities such as the Lyapunov dimension density δ, metric entropy density h, and the largest Lyapunov exponent λ_1 show that the onset of long-range spatial order (diverging ξ_2) does not affect dynamical invariants, which vary smoothly and weakly through the transition point $g = g_c$. Thus the average spatial disorder (measured by ξ_2) does not determine dynamical complexity (measured by ξ_δ). Rather surprisingly, the intensive densities δ and h go through a minimum near the transition point so that the onset of long-range order does not correspond to a decrease in complexity. By examining CMLs of different symmetry and of different dimensionality d, we showed that the positions g of the extrema were determined by the number n of neighbors nearest to a given lattice site (with $g \approx 1/(n+1)$) but not by the symmetry or by d. This result can be understood as a consequence of the extremely short dimension correlation length ξ_δ, about one lattice size, so that lattice variables are independent except when they are nearest neighbors. We believe that the minima in δ and in h occur approximately when the discrete Laplacian in Eq. (3) becomes antidiffusive with increasing parameter g. Short-wavelength fluctuations are then magnified instead of damped, decreasing correlations between neighboring sites.

Some of our results concerning extrema in dynamical quantities have been independently obtained by Boldrighini et al [30] although these authors worked with extensive, rather than intensive, quantities and they did not determine whether their calculations corresponded to

extensively chaotic regimes. Boldrighini et al investigated CMLs of the form Eq. (3) for dimensionalities $d = 1$ and $d = 2$ but with some new local maps $\phi(y)$. Besides also finding extrema in the Lyapunov fractal dimension, Boldrighini et al showed that the odd symmetry of the map $\phi(y)$ was not a sufficient condition for the magnetization to bifurcate to a nonzero value. Using a strongly chaotic local map with slope of constant magnitude equal to 5, they also showed that the magnetization M did not bifurcate to a nonzero value if the local map were made sufficiently chaotic compared to the ordering caused by diffusion. In Section III B, we used the less-chaotic local map Eq. (5) with slope of constant magnitude 1.1 to show that the dimension density δ can decrease monotonically without a minimum even when the magnetization M bifurcates to a nonzero value. The dependence of these minima on details of the local map is not yet understood and should be pursued with further studies.

The small values of ξ_δ in the present CMLs, in the 1d CGLE [12], and in a nonequilibrium CML with algebraic decay of spatial correlations [24] have several interesting implications. One is that many previous laboratory experiments [1] and numerical simulations [2] concerning spatiotemporal chaos are likely already extensive so that it is meaningful to talk about dimension and entropy densities (see also the earlier paper by Bohr [34].) A second implication is that the dimension correlation length ξ_δ may not be a useful order parameter for future studies of spatiotemporal chaos since it depends only weakly on parameters. A third implication is that the short value of ξ_δ suggests the nonexistence of macroscopic chaotic states for dynamics with local interactions, a point already made by several researchers [42]. Finally, we speculate that ξ_δ is the length scale below which one can replace chaotic fluctuations by a white noise source when trying to develop a hydrodynamic (long wavelength) description of spatiotemporal chaos (see the discussion on pages 953-954 in Ref. [7]).

The short values of ξ_δ raise the question of what determines this length scale. Our calculations on the 1d CML Eq. (10) with a variable radius of coupling r suggest that the length ξ_δ is determined partly by the length $\xi_2^{\rm mag}$ characterizing magnitude fluctuations although the reason for and the generality of this correspondence is not understood [12]. The length ξ_δ is also related to the radius r over which nearby lattice sites are coupled together

(Fig. 15). Further calculations with different kinds local maps and of diffusive operators and for different values of r should provide further insight.

It is appropriate to finish with a discussion about the relevance of these results for laboratory experiments. As discussed at the end of Section II B, it does not seem possible in the near future to calculate the Lyapunov spectrum, the fractal dimension, or the fractal dimension density of a high-dimensional extensively chaotic experimental system for which only time series measurements are available [6]. Our success in calculating these quantities was a result of having explicit knowledge of the dynamical equations which could then be integrated numerically on a powerful parallel computer using algorithms whose complexity only grew algebraically with the dimension D [37]. For many laboratory experiments, a quantitative mathematical description is either lacking (e.g., for chemical reactions) or, if known, is too difficult to work with numerically (e.g., the five three-dimensional Boussinesq equations describing buoyancy-induced convection in a large-aspect-ratio container [7]).

Our calculations in Section III suggest that one possible way to estimate the dimension correlation length ξ_δ may be to calculate the correlation length of some function of the physical fields, e.g., the field magnitude. Another possibility will be to discover and to validate algorithms that can calculate the intensive dimension density Eq. (1) directly from time-series measurements that are localized in space [43], in lieu of calculating a large extensive fractal dimension D and then dividing by the extensive system volume V. Several steps have been taken in this direction [43], but a theoretical foundation has not yet been established nor have the numerical algorithms been adequately tested.

ACKNOWLEDGEMENTS

We thank L. Bunimovich, H. Chaté, P. Hohenberg, D. Huse, H. Riecke, and J. Socolar for useful discussions. This work was supported by grants NSF-CDA-91-23483 and NSF-DMS-93-07893 of the National Science Foundation, by grant DOE-DE-FG05-94ER25214 of the Department of Energy and by an allotment of CM-5 computer time at the National

Center for Supercomputing Applications. The second author (D.A.E.) would like to thank the Office of Naval Research for fellowship support. Much of the research reported here was carried out by the first author as part of his undergraduate honors thesis in physics at Duke University.

REFERENCES

* E-mail: ohern@student.physics.upenn.edu. Present address: Department of Physics and Astonomy, University of Pennsylvania, Philadelphia, PA 19104.

† Present address: Laboratory of Atomic and Solid State Physics, Cornell University, Ithaca, NY 14850.

‡ Also Center for Nonlinear and Complex Systems and Department of Computer Science, Box 90129, Duke U., Durham, NC 27708-0129

[1] J. P. Gollub and R. Ramshankar, in *New Perspectives in Turbulence*, edited by S. Orszag and L. Sirovich (Springer-Verlag, Berlin, 1990), pp. 165–194; S. W. Morris, E. Bodenschatz, D. S. Cannell, and G. Ahlers, Phys. Rev. Lett. **71**, 2026 (1993); M. Assenheimer and V. Steinberg, Nature **367**, 345 (1994); F. T. Arecchi *et al.*, Physica D **61**, 25 (1992); Q. Ouyang and H. L. Swinney, Chaos **1**, 411 (1991).

[2] B. I. Shraiman *et al.*, Physica D **57**, 241 (1992); H.-W. Xi, J. D. Gunton, and J. Viñals, Phys. Rev. Lett. **71**, 2030 (1993); J. E. Pearson, Science **261**, 189 (1993); D. A. Egolf and H. S. Greenside, Nature **369**, 129 (1994); W. Decker, W. Pesch, and A. Weber, Phys. Rev. Lett. **73**, 648 (1994); M. Cross, D. Meiron, and Y. Tu, Chaos **4**, (1994).

[3] M. C. Cross and P. C. Hohenberg, Science **263**, 1569 (1994).

[4] P. C. Hohenberg and B. I. Shraiman, Physica D **37**, 109 (1989).

[5] E. Ott, *Chaos in Dynamical Systems* (Cambridge U. Press, New York, 1993).

[6] N. A. Gershenfeld, Physica D **55**, 135 (1992); J.-P. Eckmann and D. Ruelle, Physica D **56**, 185 (1992).

[7] M. C. Cross and P. C. Hohenberg, Rev. Mod. Phys. **65**, 851 (1993).

[8] P. Coullet, L. Gil, and J. Lega, Phys. Rev. Lett. **62**, 1619 (1989).

[9] K. Nozaki and N. Bekki, J. Phys. Soc. Jpn **53**, 1581 (1984).

[10] H. Sakaguchi, Prog. Theor. Phys. **80**, 7 (1988).

[11] B. I. Shraiman *et al.*, Physica D **57**, 241 (1992).

[12] D. A. Egolf and H. S. Greenside, Phys. Rev. Lett. **74**, 1751 (1995).

[13] H. Sakaguchi, Prog. Theor. Phys. **86**, 303 (1991).

[14] J. Miller and D. A. Huse, Phys. Rev. E **48**, 2528 (1993).

[15] S. W. Morris, E. Bodenschatz, D. S. Cannell, and G. Ahlers, Phys. Rev. Lett. **71**, 2026 (1993); M. Assenheimer and V. Steinberg, Phys. Rev. Lett. **70**, 3888 (1993); W. Decker, W. Pesch, and A. Weber, Phys. Rev. Lett. **73**, 648 (1994).

[16] H. Chaté, Europhys. Lett. **21**, 419 (1993).

[17] D. A. Egolf and H. S. Greenside, Nature **369**, 129 (1994).

[18] V. S. Afraimovich and L. A. Bunimovich, Physica D **80**, 277 (1995).

[19] D. A. Egolf, Ph.D. thesis, Duke University, Department of Physics, Duke University, Durham, NC, 1994.

[20] P. Manneville, in *Macroscopic Modeling of Turbulent Flows*, O. Pironneau ed., *Lecture Notes in Physics* **230** (Springer-Verlag, New York, 1985), pp. 319.

[21] P. Grassberger, Phys. Scripta **40**, 346 (1989).

[22] L. Sirovich and A. E. Deane, J. Fluid Mech. **222**, 251 (1991); L. Keefe, P. Moin, and J. Kim, J. Fluid Mech. **242**, 1 (1992).

[23] W. van de Water and T. Bohr, Chaos **3**, 747 (1993).

[24] C. O'Hern, D. Egolf, and H. Greenside, in preparation.

[25] H. Chaté, in *Spatio-Temporal patterns in Nonequilibrium Complex Systems*, Vol. XXI of *Santa Fe Institute Studies in the Science of Complexity*, Santa Fe Institute, edited by

P. E. Cladis and P. Palffy-Muhoray (Addison-Wesley, Reading, Massachusetts, 1995), pp. 33–50.

[26] W. D. Hillis and B. M. Boghosian, Science **261**, 856 (1993).

[27] L. A. Bunimovich and Y. G. Sinai, Nonlinearity **1**, 491 (1988).

[28] P. Marcq and H. Chate, private communication.

[29] L. Landau and E. Lifshitz, *Statistical Physics*, Third ed. (Pergamon, New York, 1980), Vol. 5, Part 1.

[30] C. Boldrighini *et al.*, submitted to J. Stat. Phys. (1995).

[31] D. Egolf and C. O'Hern, in preparation.

[32] T. S. Parker and L. O. Chua, *Practical Numerical Algorithms for Chaotic Systems* (Springer-Verlag, New York, 1989).

[33] I. Goldhirsch, P.-L. Sulem, and S. A. Orszag, Physica D **27**, 311 (1994).

[34] T. Bohr and O. Christensen, Phys. Rev. Lett. **63**, 2161 (1989).

[35] C. D. Cutler, Commun. Math. Phys. **129**, 621 (1990).

[36] H. D. Abarbanel, R. Brown, and L. S. Tsimring, Rev. Mod. Phys. **65**, 1331 (1993).

[37] For a numerical dynamical model with N independent variables, an optimal integration scheme will advance the variables in one time step with a computational effort that grows at best as slowly as $O(N)$. Each linearized equation also involves N variables and so the effort needed to calculate K Lyapunov exponents by the algorithm discussed in Section II over a fixed time time T will grow at best as slowly as $O(TKN)$. Since the number of exponents needed to estimate the Lyapunov dimension grows linearly with system volume, as does the number N itself, we conclude that the computational effort to calculate the Lyapunov dimension for an extensively chaotic system, for an

observation time T, will grow at best as slowly as $O(TN^2)$, i.e., algebraically with N. It is presently not understood how the total integration time T should itself scale with system volume or with N and so the exponent of the algebraic scaling with dimension D is not yet known [31].

[38] N. J. I. Mars and G. W. van Arragon, Signal Processing **4**, 139 (1982); A. M. Fraser and H. L. Swinney, Phys. Rev. A **33**, 1134 (1986); A. M. Fraser, IEEE Trans. Info. Theory **35**, 245 (1989).

[39] F. Reif, *Fundamentals of Statistical and Thermal Physics* (McGraw-Hill, New York, 1965).

[40] J. A. Vastano and H. L. Swinney, Phys. Rev. Lett. **60**, 1773 (1988).

[41] E. Bosch, H. Lambermont, and W. van de Water, Phys. Rev. E **49**, 3580 (1994).

[42] T. Bohr, G. Grinstein, Y. He, and C. Jayaprakash, Phys. Rev. Lett. **58**, 2155 (1987); H. Chaté and P. Manneville, Prog. Theor. Phys. **87**, 1 (1992).

[43] Y. Pomeau, Acad. Sci. Paris **300**, Ser. II, 239 (1985); P. Grassberger Phys. Scripta **40**, 346 (1989); A. Torcini, A. Politi, G. P. Puccioni, and G. D'Alessendro, Physica D **53**, 85 (1991); L. S. Tsimring, Phys. Rev. E **48**, 3421 (1993); M. Bauer, H. Heng, and W. Martienssen, Phys. Rev. Lett. **71**, 521 (1993).

FIGURES

FIG. 1. Lyapunov fractal dimension D, Eq. (6), versus iteration number t for a periodic 2d CML on a square lattice with local map Eq. (4), with coupling constant $g = 0.202$ and with lattice size $L = 16$. Fluctuations in D damp out slowly with increasing time, giving a relative accuracy of about 0.1% in the dimension (here estimated to be $D = 191.2$).

FIG. 2. Lyapunov fractal dimension D versus the number of lattice points $N = L^2$ (which is also the system volume) for a 2d periodic CML on a square lattice with local map Eq. (4) and coupling constant $g = 0.199$. Each dimension value was obtained from a plot similar to Fig. 1 over a time scale of $T = 50,000$ iterations. **(a)** The Lyapunov dimension increases linearly and so extensively with N for $N > 100$. A least-squares fitted line through the four right-most points gives a Lyapunov dimension density (slope) of $\delta = 0.746$ and an intercept of 0.0077. **(b)** The normalized deviation $(D/L^2 - \delta)/\delta$ of the dimension density δ from the dimension density predicted from the dimension D per volume L^2 illustrates the rapid onset of extensive chaos for small system sizes $L > 9$.

FIG. 3. Average magnetization M (Eq. (8)) versus the lattice coupling strength g for a two-dimensional CML with local map Eq. (4) on a square lattice of size $L = 128$ after an integration time of $T = 3 \times 10^5$. The magnetization bifurcates from a nonzero value at the critical value $g_c = 0.205$.

FIG. 4. Log-linear plot of the exponentially decaying two-point correlation function Eq. (9) of the two-dimensional CML Eq. (3) with local map Eq. (4) on a square lattice for lattice sizes of $L = 64, \cdots, 1024$. The coupling constant was $g = 0.199$ and the integration time was $T = 3 \times 10^5$. A reasonably accurate estimate of the correlation length $\xi_2 \simeq 6$ is found only for sizes $L \geq 256$. The arrows indicate the range over which a least-squares linear fit was used to extract the length ξ_2.

FIG. 5. Plot of the two-point correlation function Eq. (9) for the magnitudes $|y_i^t|$ of the field for the 2d periodic CML with local map Eq. (4) on a square lattice with $g = 0.200$. A system size $L = 64$ and an integration time of $T = 5 \times 10^5$ were used. The correlation length $\xi_2^{\rm mag} \approx 1.4$ is smaller than the length $\xi_2 \approx 6$ based on the values y_i^t.

FIG. 6. Log-linear plot showing the exponential decay of the mutual information function $I(\triangle x)$ as a function of the spatial separation $\triangle x$ for the 2d periodic CML on a square lattice with local map Eq. (4), coupling constant $g = 0.204$, system size $L = 256$, and effective integration time $T = 128,000$ (following a transient time of $100,000$). The arrows indicate the range over which a linear least-squares fit was used to calculate the correlation length $\xi_I \approx 11.7$. A simple binning procedure with 32 bins was adequate so that the more sophisticated algorithms of Fraser et al [38] were not needed.

FIG. 7. Two-point correlation length ξ_2 versus the mutual information correlation length ξ_I for a 2d periodic CML on a square lattice with local map Eq. (4). Lattices sizes of $L = 1024$ and $L = 256$ and integration times of $T = 300,000$ and $T = 128,000$ were used respectively when calculating ξ_2 and ξ_I. The points correspond to the parameter range $0.1900 \leq g \leq 0.2045$ with the smaller g values occurring to the left. The values of ξ_2 and ξ_I were obtained from plots similar to Fig. 4 and Fig. 6

FIG. 8. **(a)** Divergence of ξ_2 for the 2d periodic CML on a square lattice with local map Eq. (4). The lattice size was $L = 1024$ and the integration time was $T = 3 \times 10^5$ based on an ensemble average over 64 realizations. The correlation length diverges with critical exponent ≈ -1.0 at the extrapolated point $g = 0.2054$ which coincides within numerical accuracy with the pitchfork bifurcation of the magnetization. **(b)** The dimension correlation length ξ_δ (Eq. (2)) versus parameter g for the same parameter values, based on dimension densities calculated from extensive chaos curves like Fig. 2. This length scale is roughly one lattice size, varies smoothly with g, and attains a maximum value for $g \approx 0.200$.

FIG. 9. Lyapunov exponents λ_i versus the intensive index $x = i/L^2$ for the 2d periodic CML on a square lattice with local map Eq. (4) for the lattice size $L = 24$, for an integration time $T = 50,000$, and for lattice coupling values $g = 0.19$ and $g = 0.22$ which straddle the transition at $g = 0.205$. The exponents form an approximately continuous function that changes smoothly with parameter g. Only the first 512 of the 576 possible exponents are shown.

FIG. 10. **(a)** The Lyapunov fractal dimension density δ, **(b)** the entropy density h, and **(c)** the largest Lyapunov exponent λ_1 versus the coupling constant g in the vicinity of the ferromagnetic transition of $g_c = 0.205$ according to the magnetization curve in Fig. 3 for the 2d CML on a square lattice with local map Eq. (4). System sizes of at least $L = 16$ were used with a fixed integration time $T = 5 \times 10^4$ and an ensemble average over $p = 64$ systems. The quantities δ and h have local minima (although at slightly different g values) to the left of where the magnetization bifurcates. The error bars of each data point are about the size of the points themselves except for those of λ_1 which are much larger.

FIG. 11. Magnetization M (Eq. (8)) versus coupling strength g for the 2d periodic CML on a square lattice but with the less chaotic lattice map given by Eq. (5). Other parameter values were the sizes, $L = 64$ and $L = 128$ and the total integration time, $T = 3 \times 10^5$. The bifurcation occurs at approximately $g_c \approx 0.168$.

FIG. 12. Lyapunov dimension density δ and entropy density h versus coupling constant g for the 2d periodic CML with local map Eq. (5), for lattice size $L = 32$ and for an integration time $T = 10^4$. The largest Lyapunov exponent $\lambda_1 = 0.095$ remains constant in the range $0.160 < g < 0.180$ and so is not plotted. For this substantially less chaotic local map, extrema in the dynamical quantities do not occur.

FIG. 13. **(a)** Magnetization M (Eq. (8)) versus coupling strength g for 2d periodic CML on a hexagonal lattice with local map Eq. (4), with integration time $T = 1 \times 10^5$ time units, for a system size $L = 64$, and for an ensemble average of $p = 64$ elements. A ferromagnetic transition occurs at $g = g_c \approx 0.12$. **(b)** Dimension correlation length ξ_δ versus the lattice coupling constant g for the same parameters except with a system size $L = 16$ and integration time $T = 5 \times 10^4$. The maximum in ξ_δ does not coincide with the bifurcation of the magnetization in **(a)**. Over this range, the Lyapunov dimension decreases from a value of 106 to a minimum of $D \approx 100$ at $g = 0.14$.

FIG. 14. **(a)** Magnetization M (Eq. (8)) versus lattice coupling strength g for the 3d periodic CML with local map Eq. (4) on a cubic lattice. A system size of $L = 16$, a total integration time of $T = 1 \times 10^5$ time units, and an ensemble average of $p = 64$ realizations were used. The magnetization bifurcates to a nonzero value at $g = g_c \approx 0.11$. **(b)** The dimension correlation length ξ_δ versus g for the same parameters, calculated on a lattice of size $L = 6$ and for a time of $T = 1 \times 10^4$ time units. The corresponding dimension D varies from 120 down to a minimum of about 105 at $g = 0.15$.

FIG. 15. Variation of the correlation length ξ_2, the correlation length of magnitude fluctuations ξ_2^{mag}, and the dimension correlation length ξ_δ with the radius of spatial coupling r for the 1d periodic CML Eq. (10) with local map Eq. (4). The system sizes ranged from $L = 64$ to $L = 1024$ with larger systems being used for larger radii. The integration time was $T = 300,000$ for all systems. The length $\xi_\delta \approx 5.3$ for $r = 5$ is substantially larger than the maximum value of $\xi_\delta \approx 1.2$ found for the 2d Miller-Huse CML with nearest neighbor coupling.

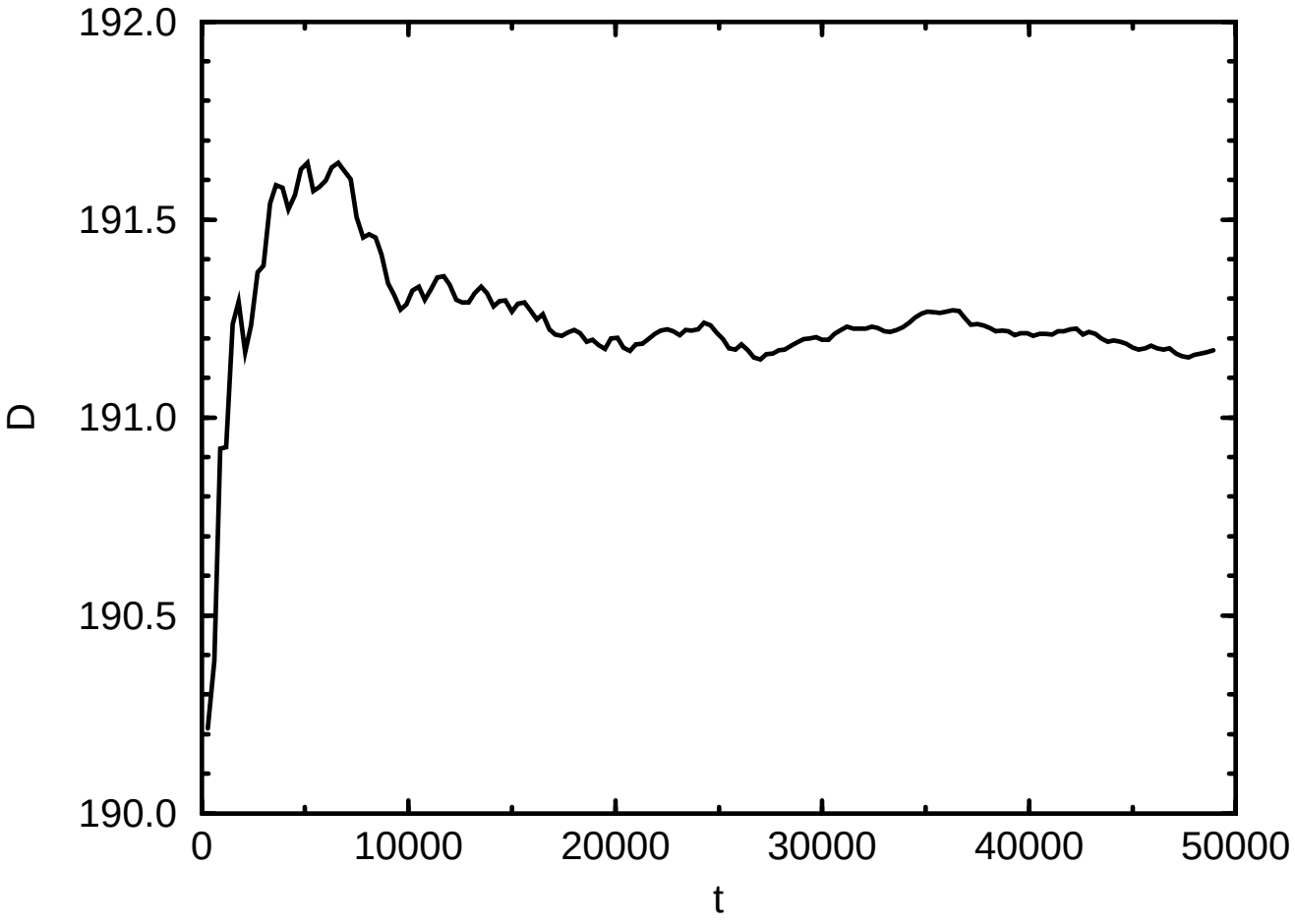

Figure 1. O'Hern et al. Lyapunov Spectral Analysis...

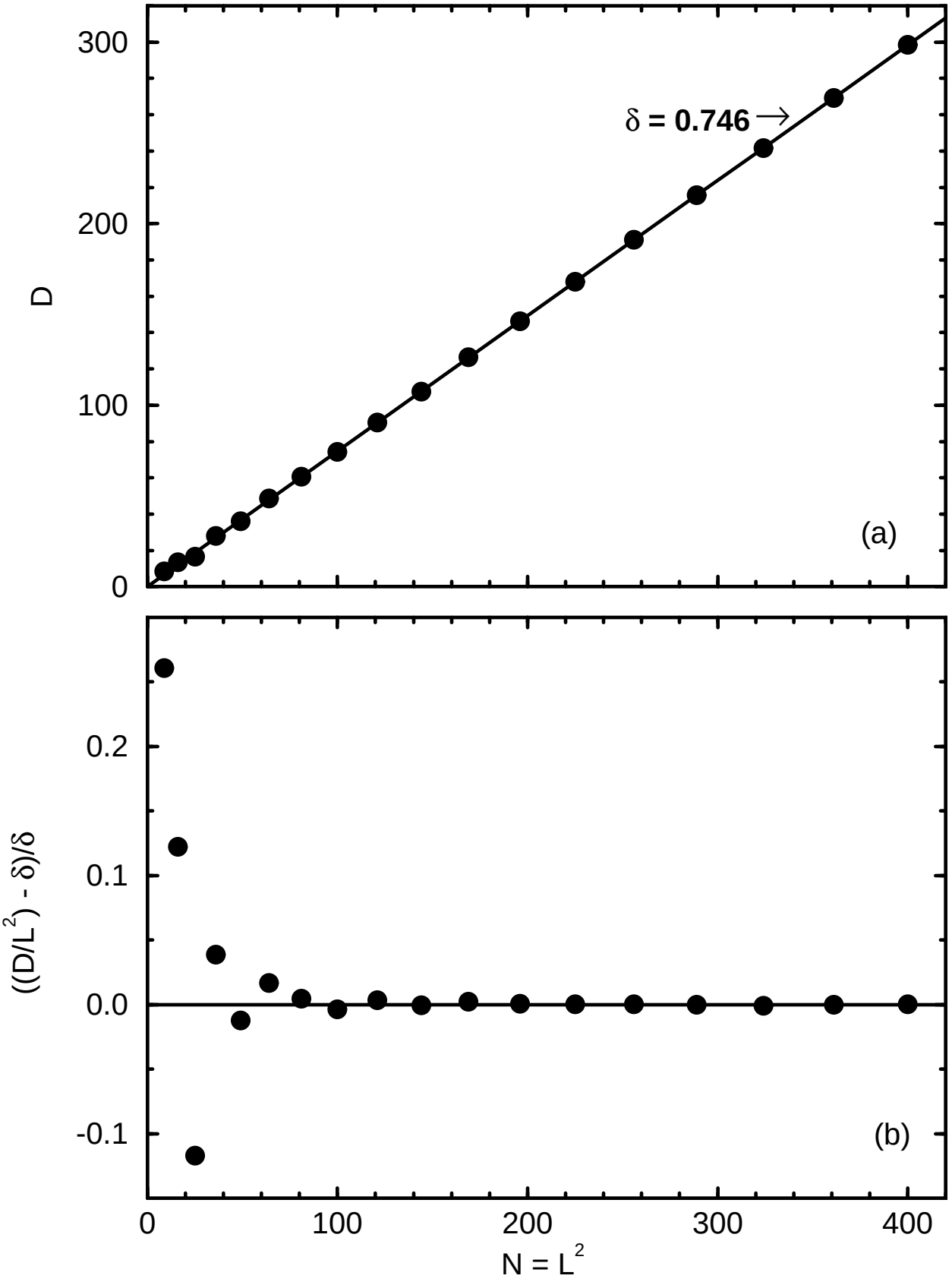

Figure 2. O'Hern et al. Lyapunov Spectral Analysis...

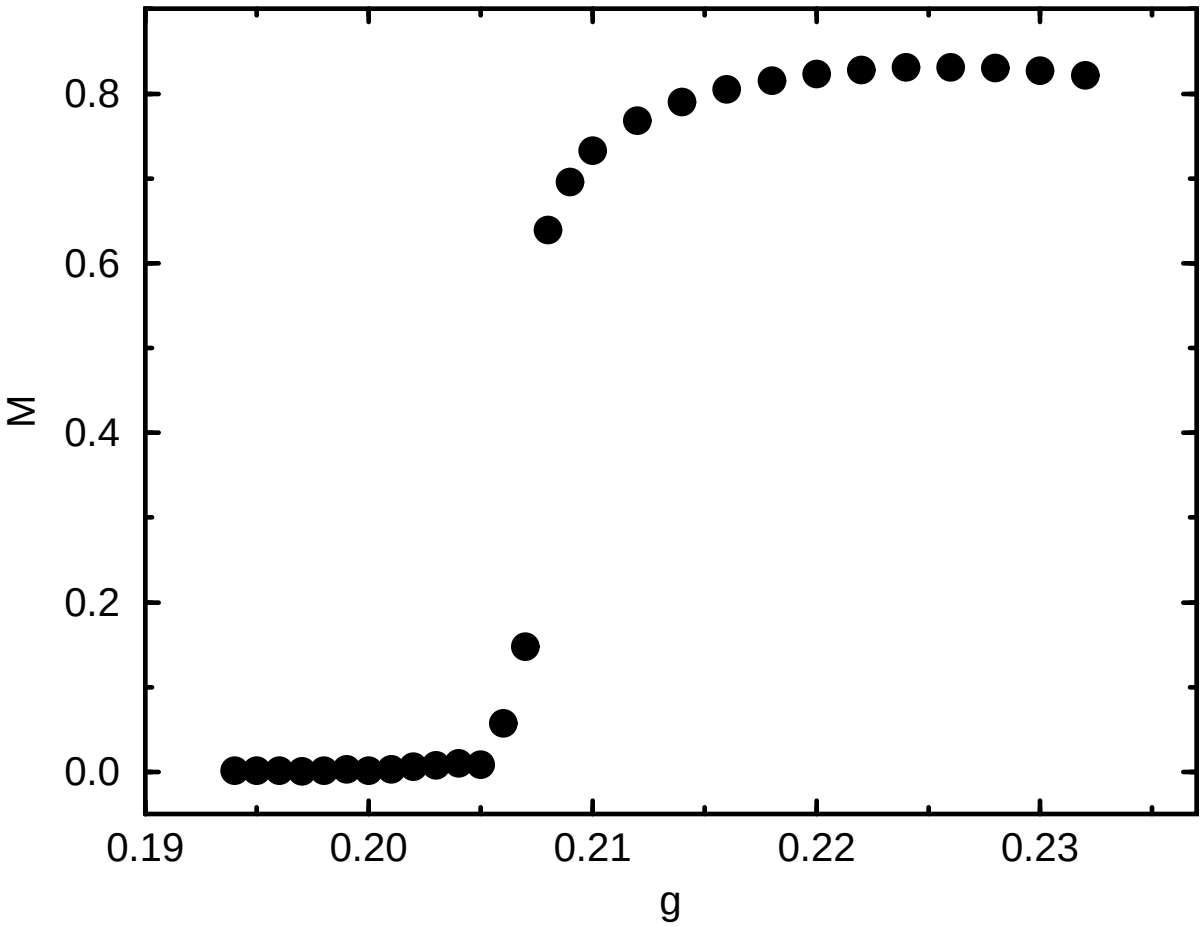

Figure 3. O'Hern et al. Lyapunov Spectral Analysis...

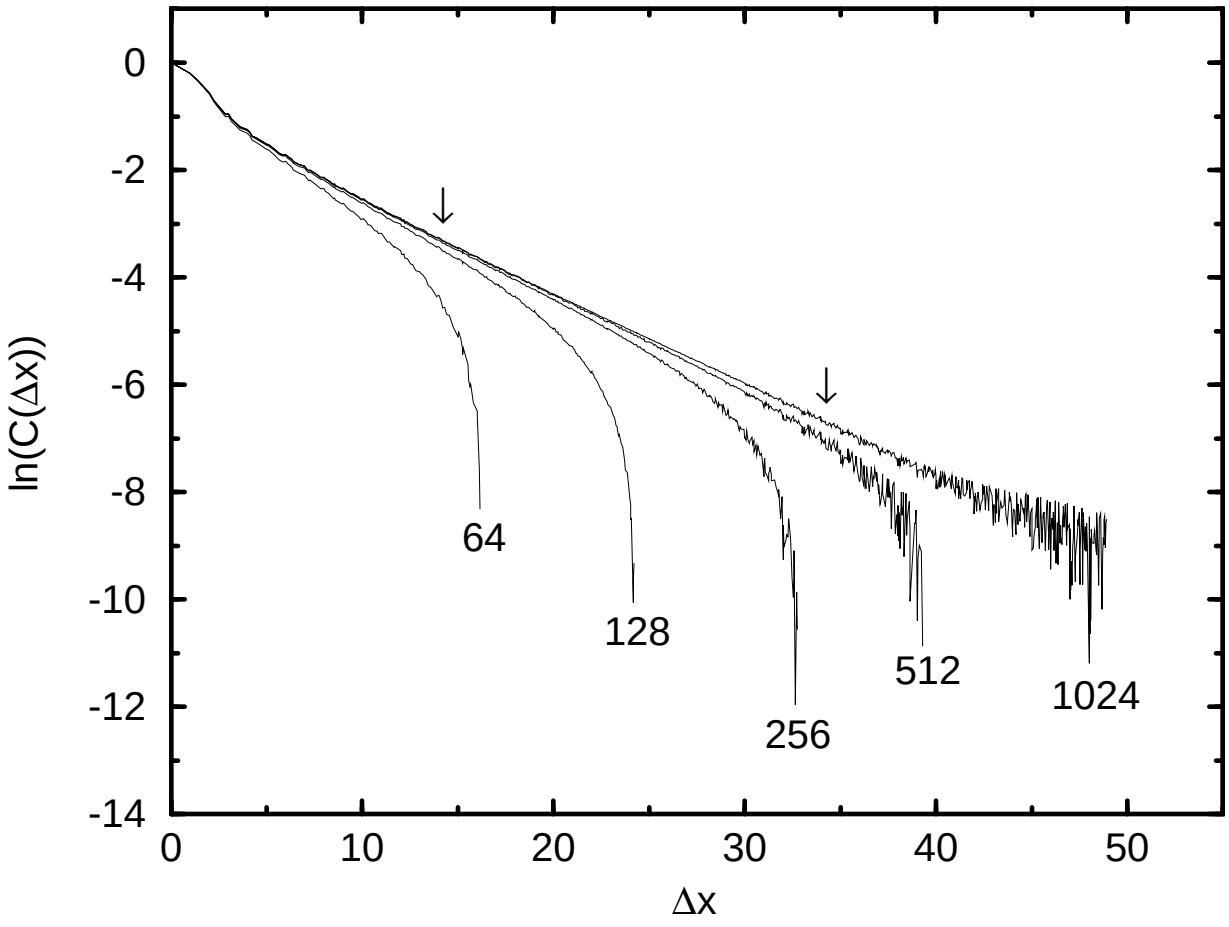

Figure 4. O'Hern et al. Lyapunov Spectral Analysis...

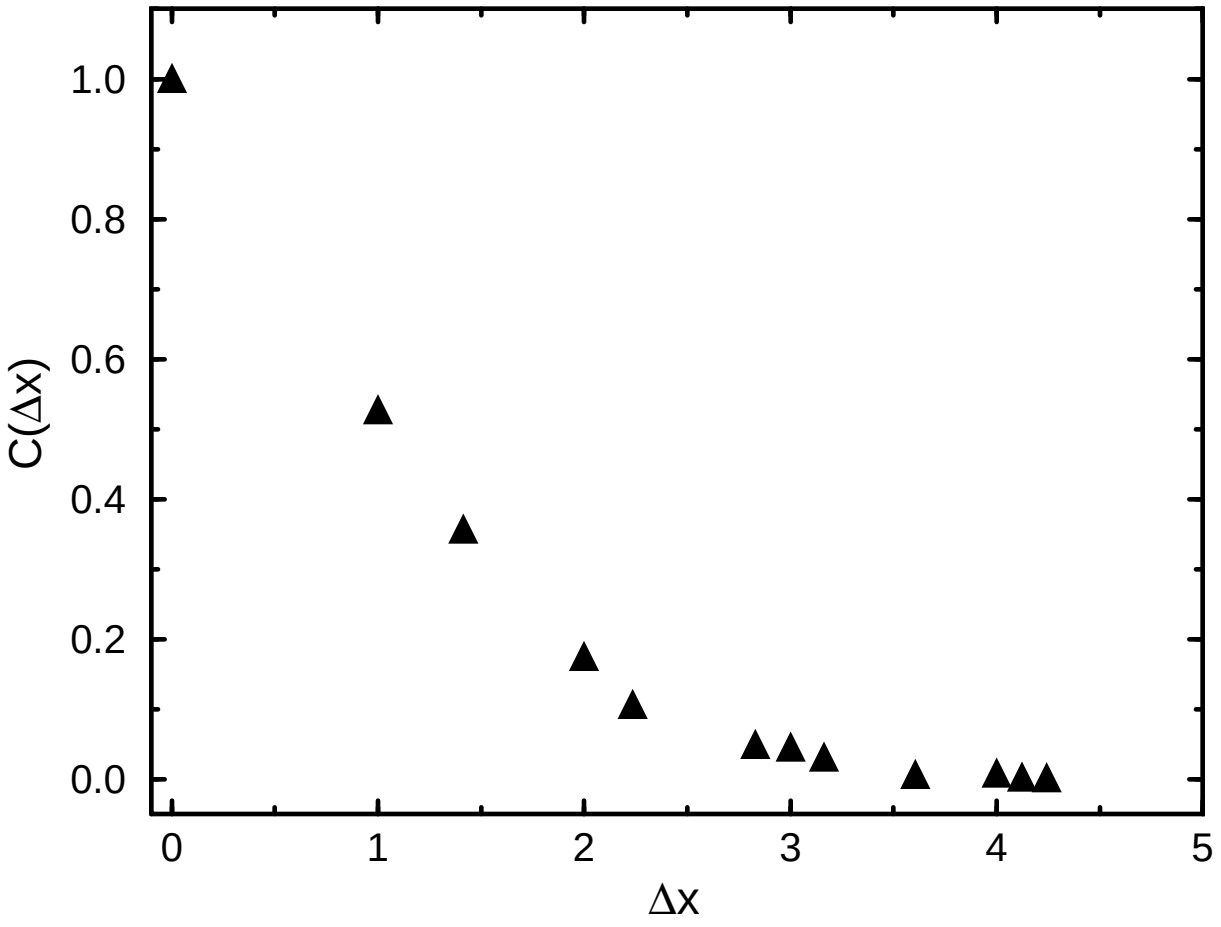

Figure 5. O'Hern et al. Lyapunov Spectral Analysis...

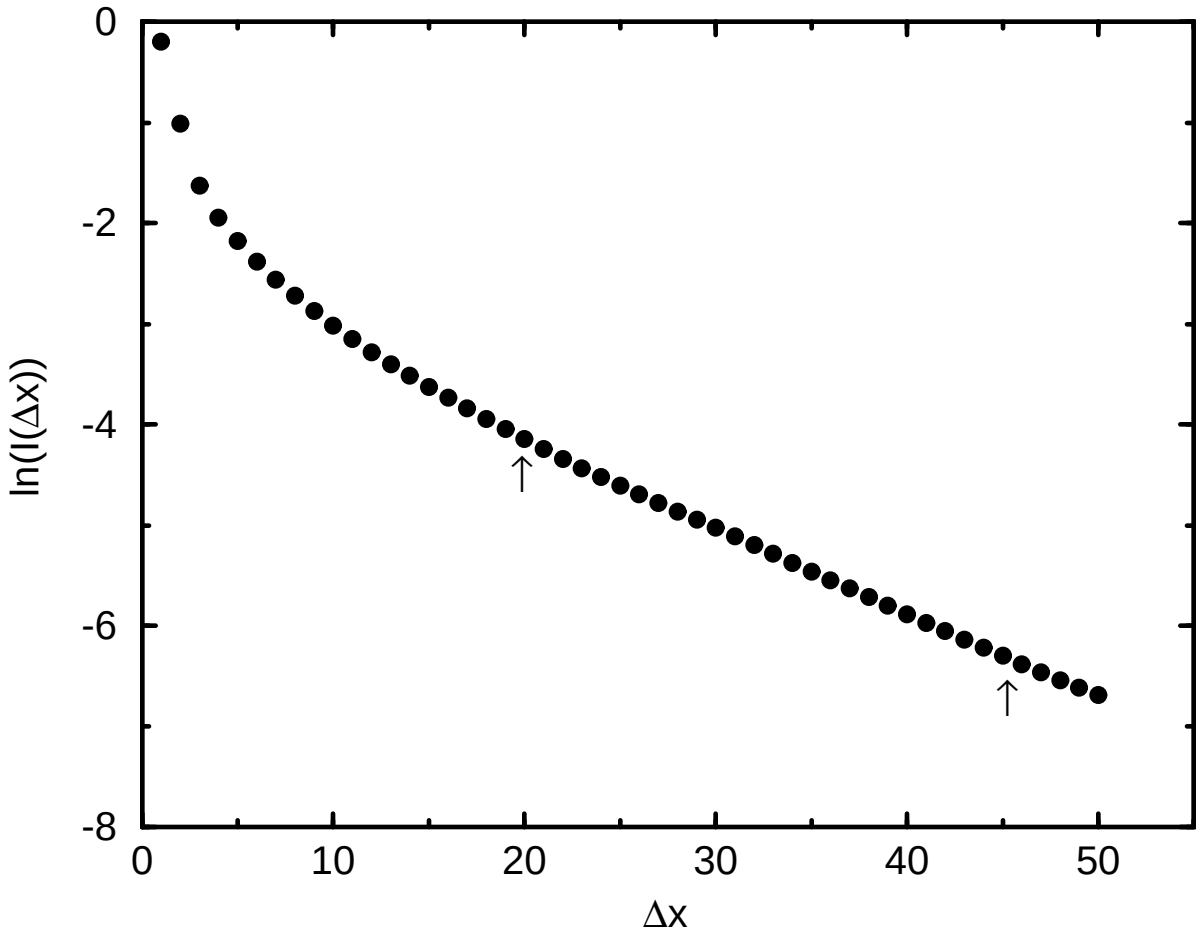

Figure 6. O'Hern et al. Lyapunov Spectral Analysis...

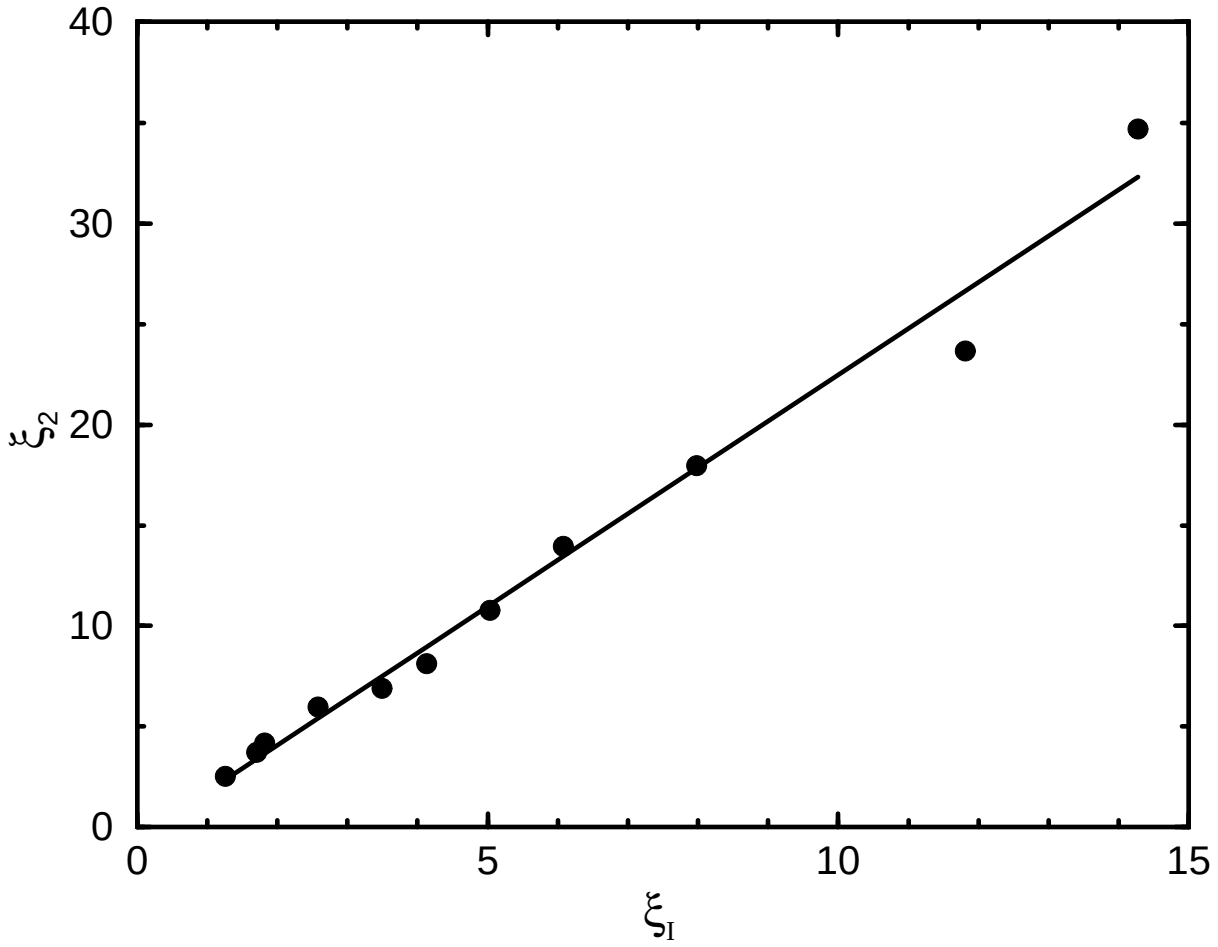

Figure 7. O'Hern et al. Lyapunov Spectral Analysis...

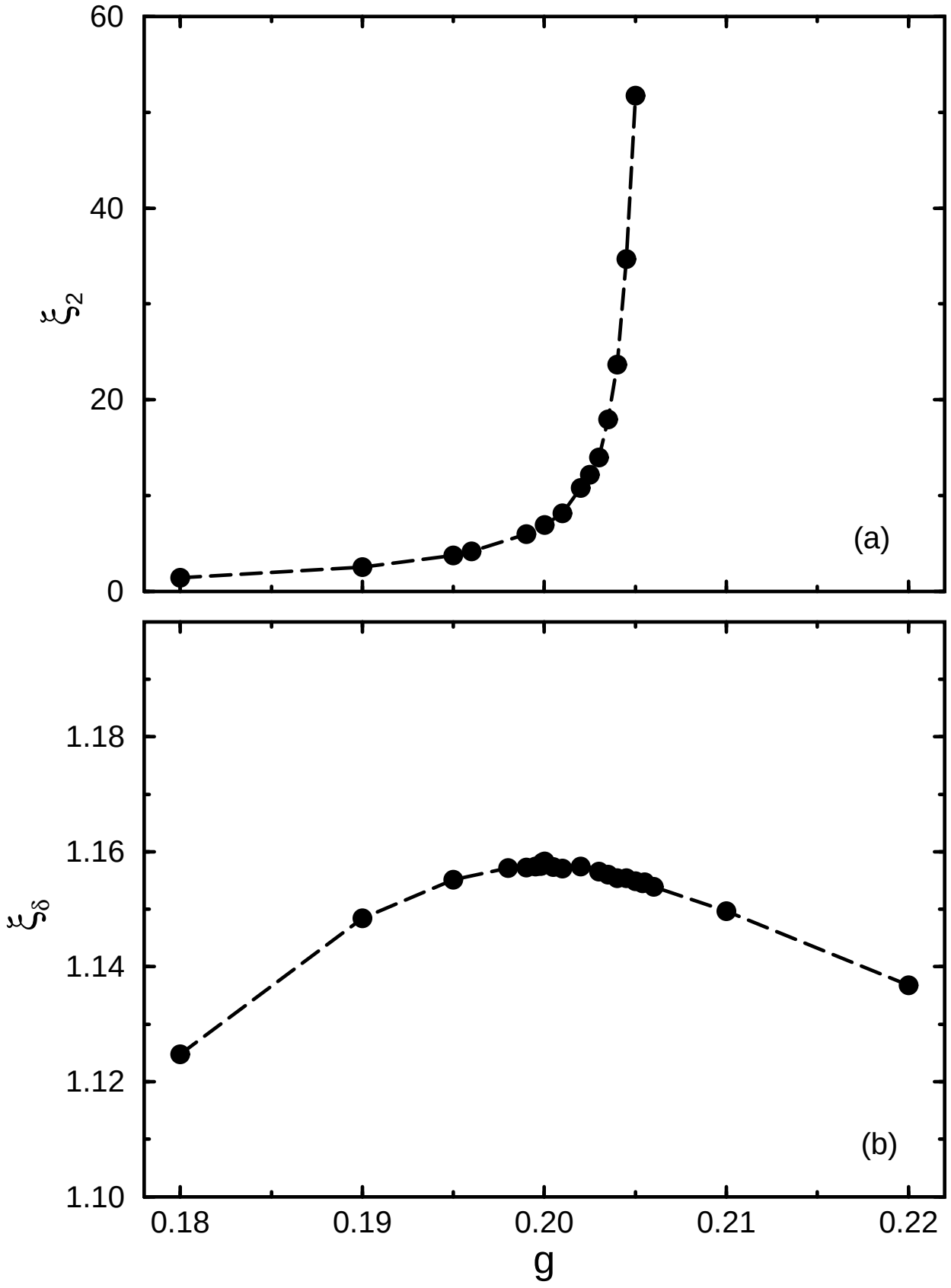

Figure 8. O'Hern et al. Lyapunov Spectral Analysis...

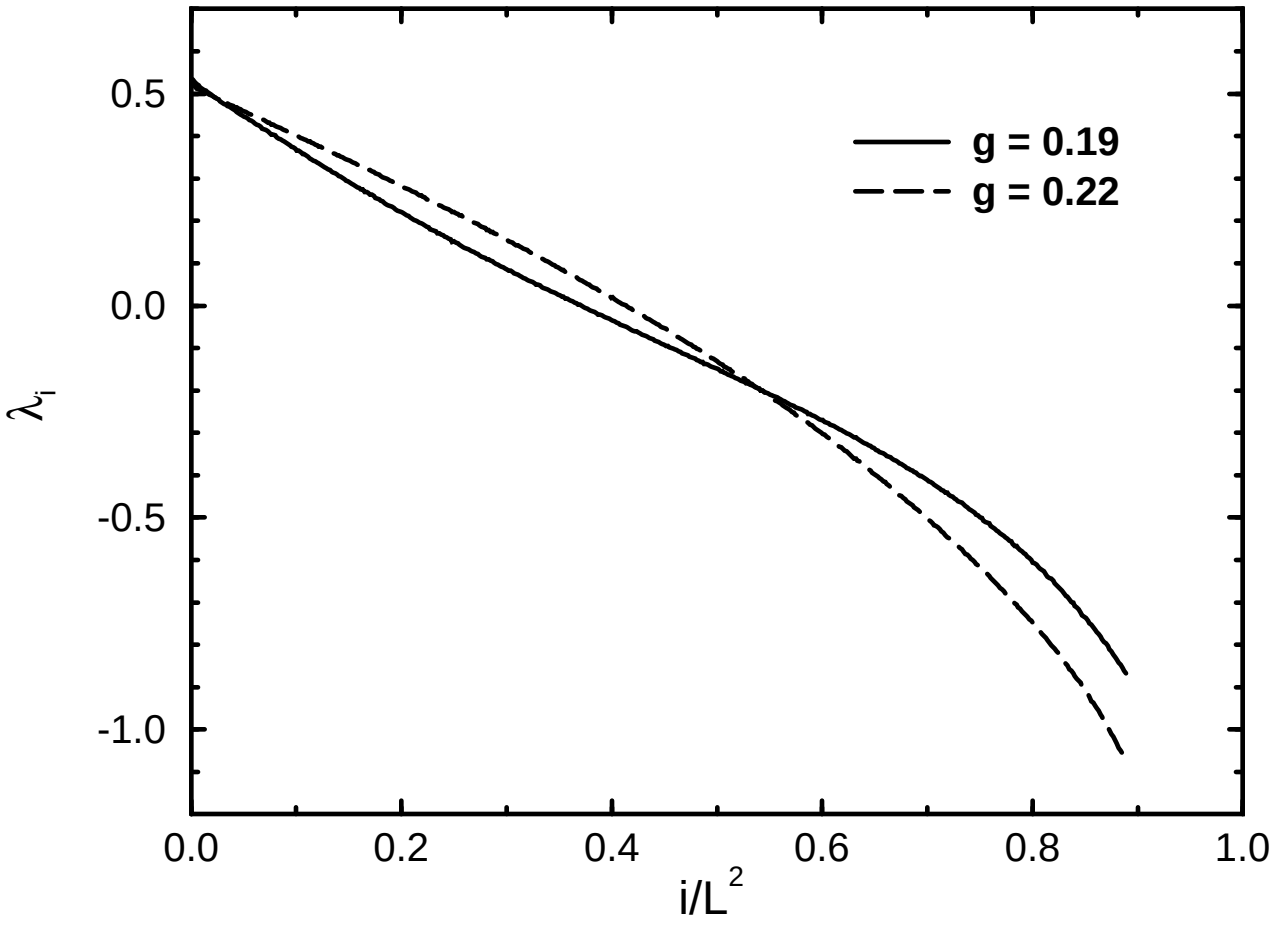

Figure 9. O'Hern et al. Lyapunov Spectral Analysis...

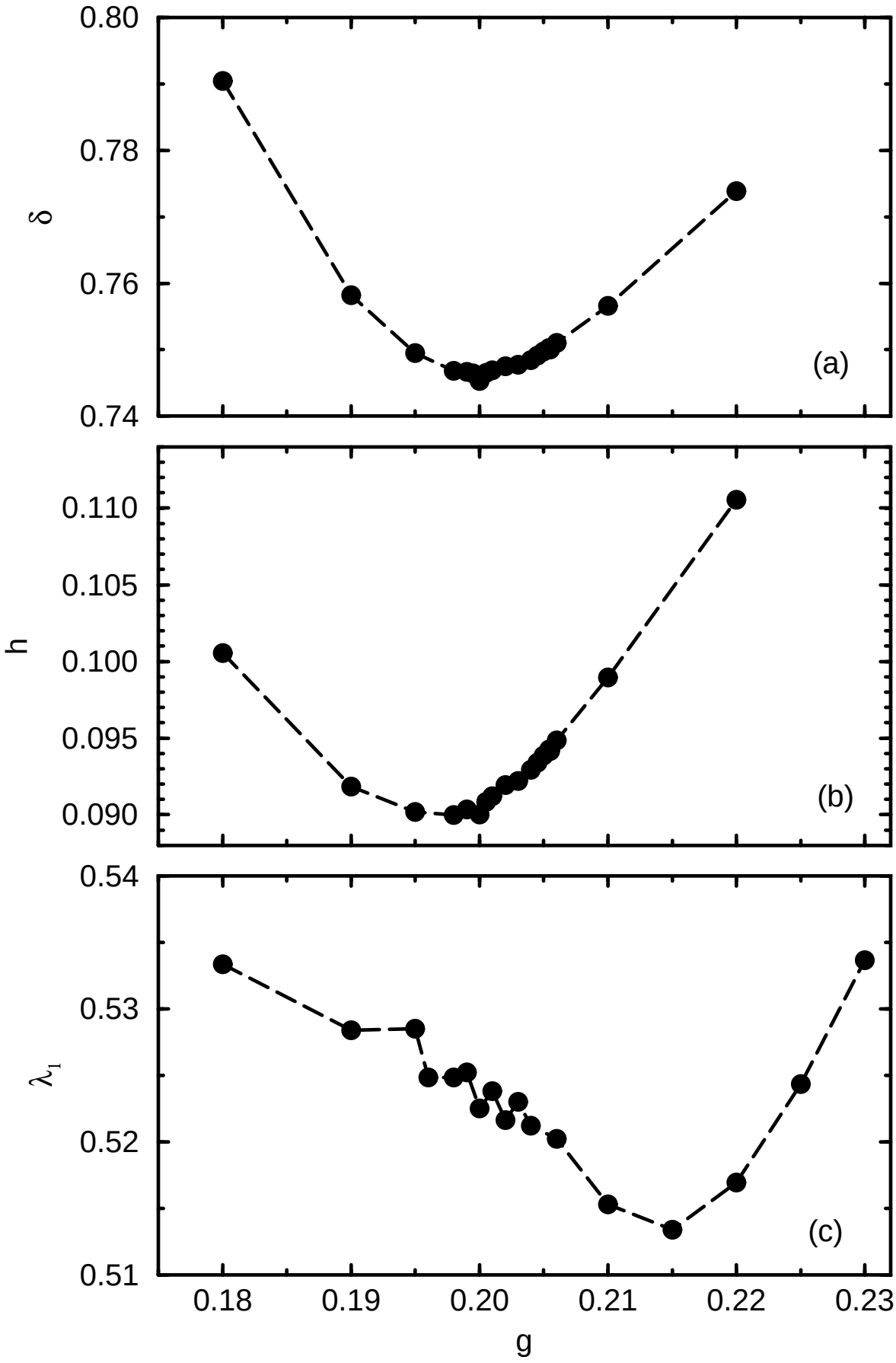

Figure 10. O'Hern et al. Lyapunov Spectral Analysis...

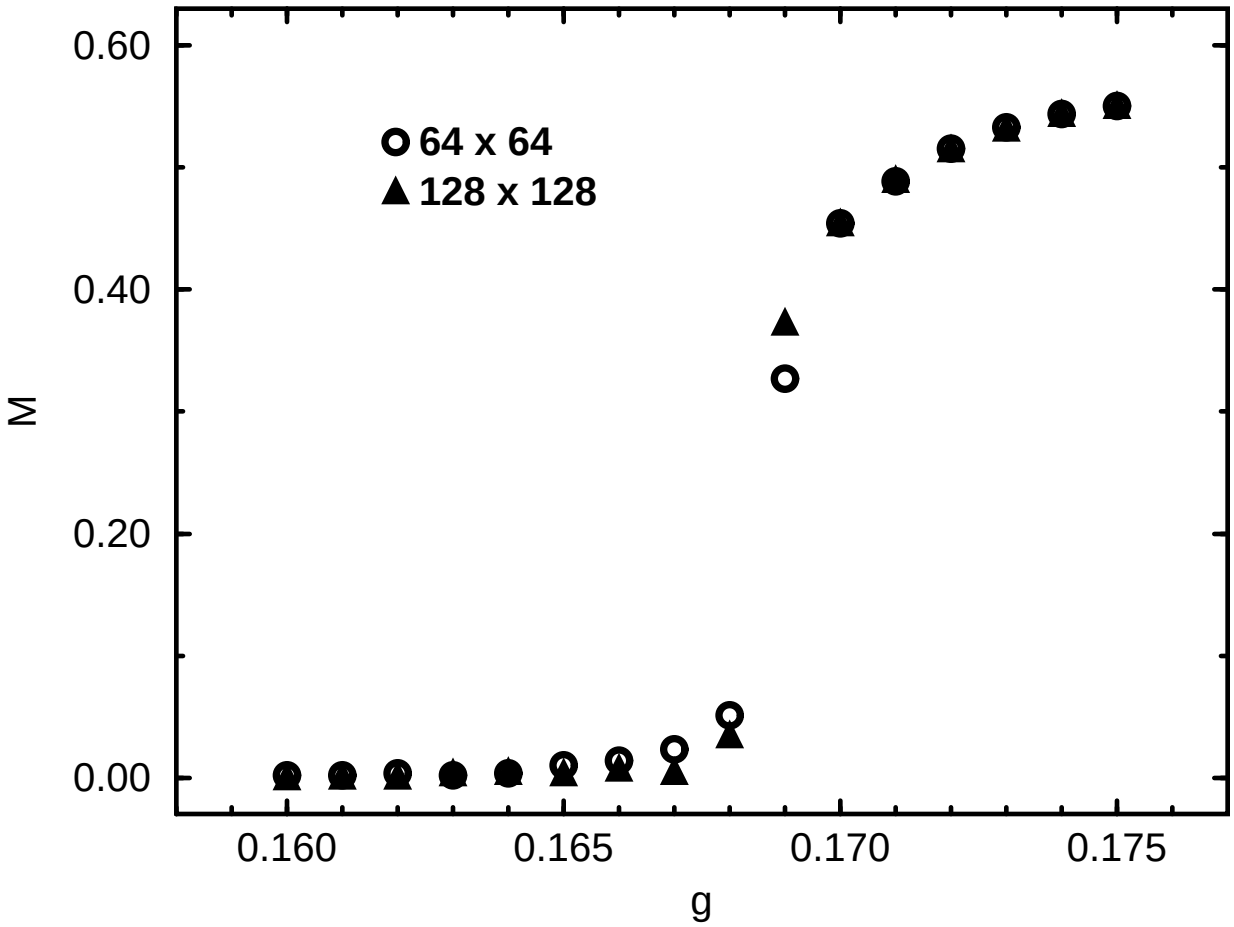

Figure 11. O'Hern et al. Lyapunov Spectral Analysis...

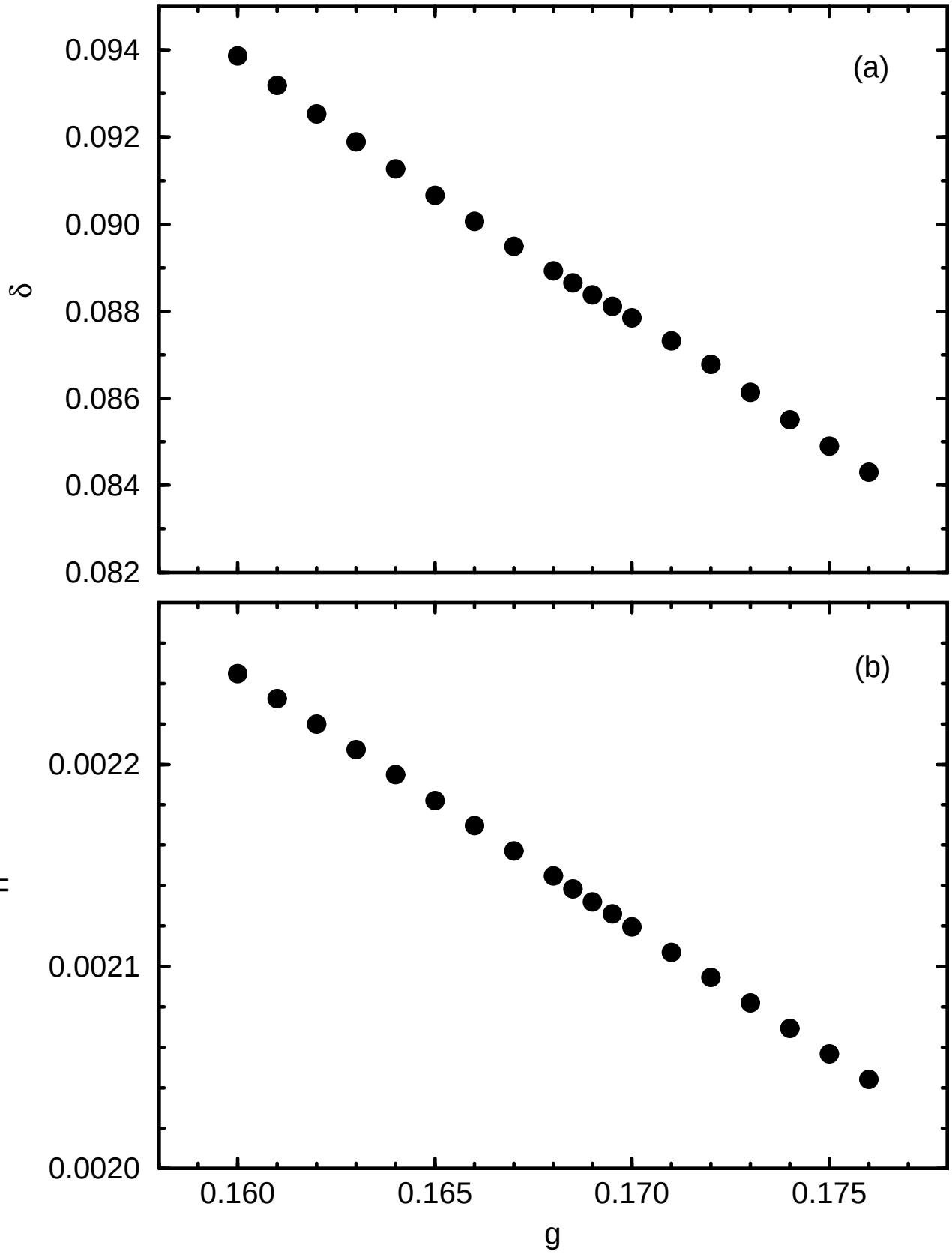

Figure 12. O'Hern et al. Lyapunov Spectral Analysis...

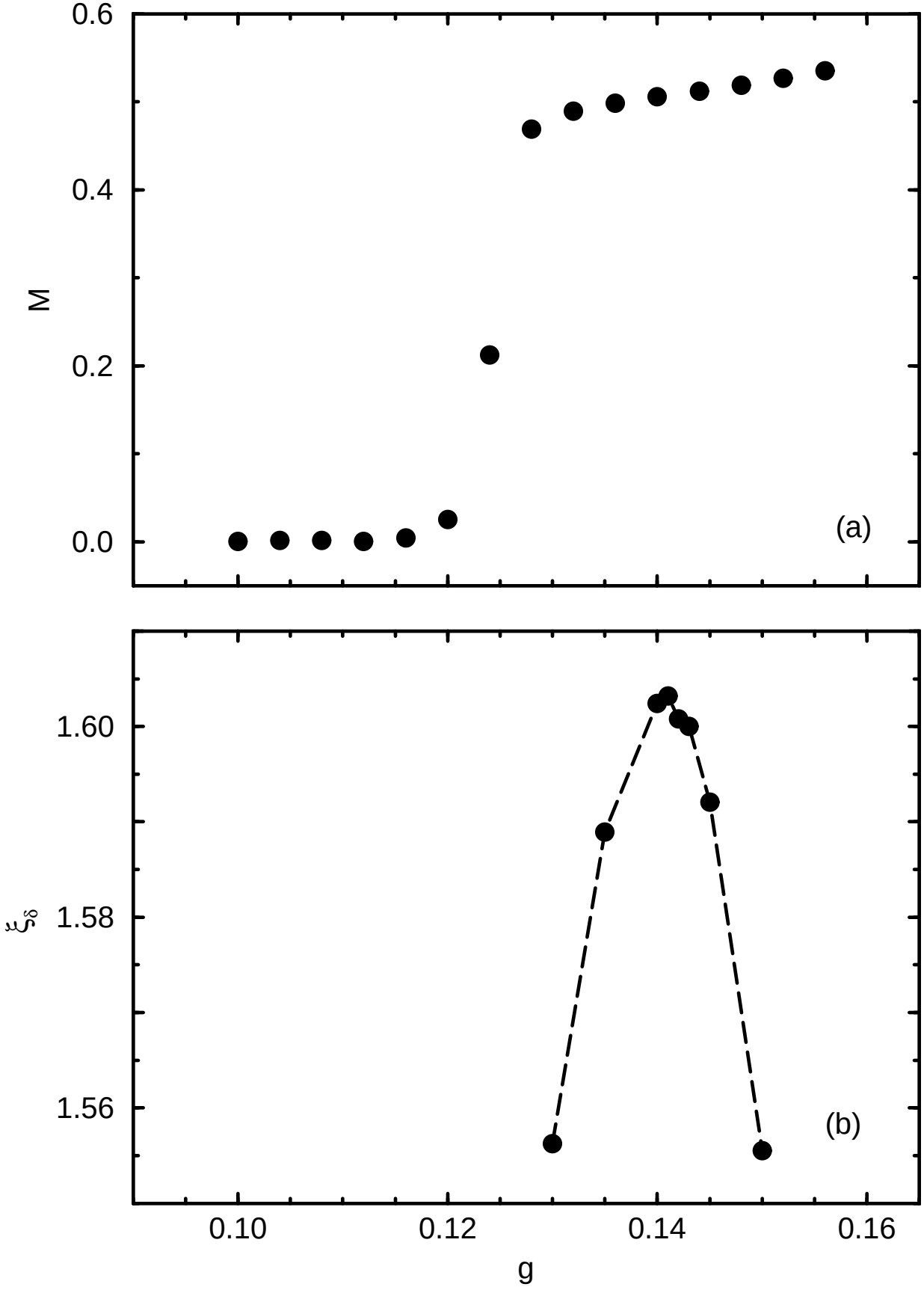

Figure 13. O'Hern et al. Lyapunov Spectral Analysis...

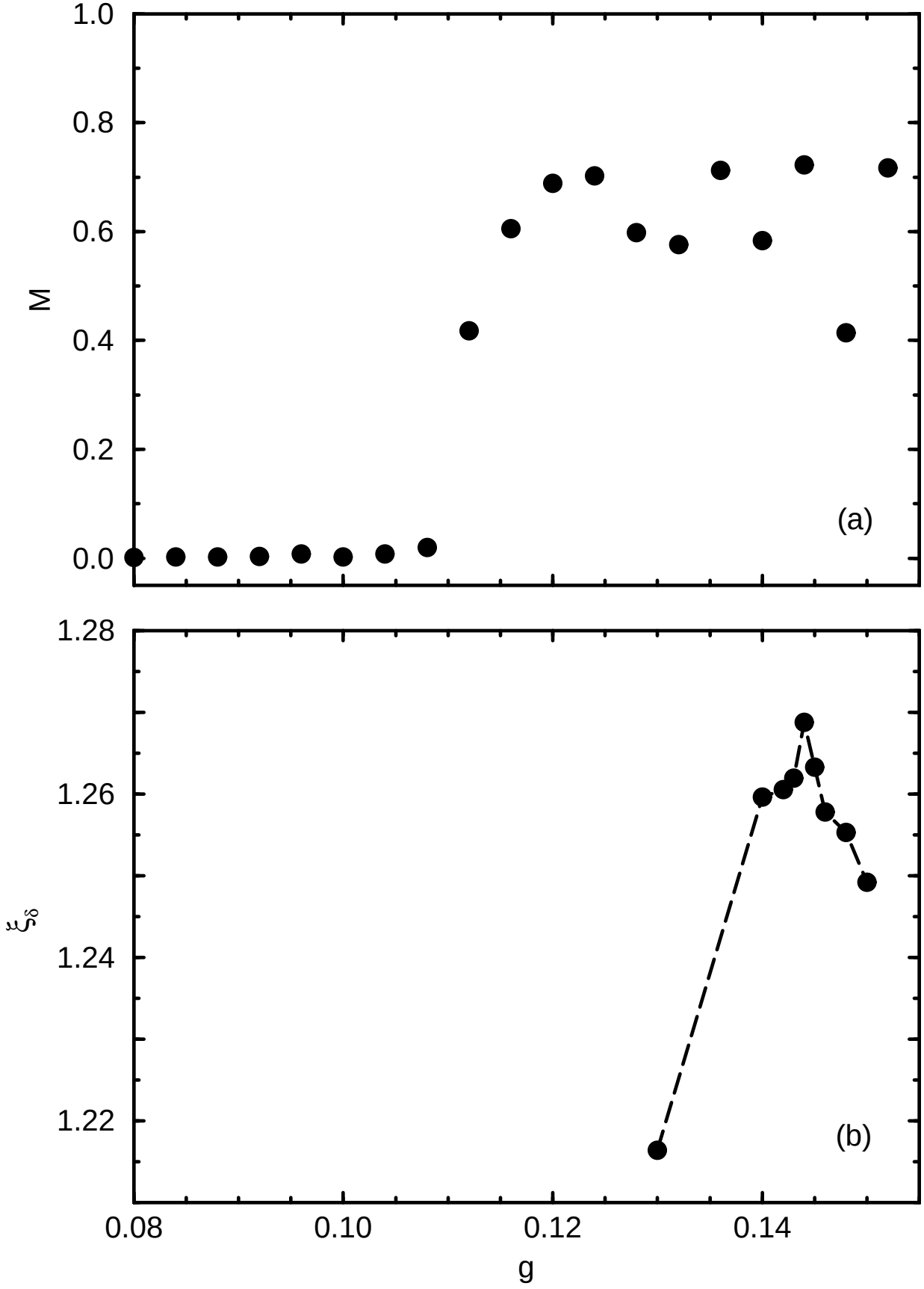

Figure 14. O'Hern et al. Lyapunov Spectral Analysis...

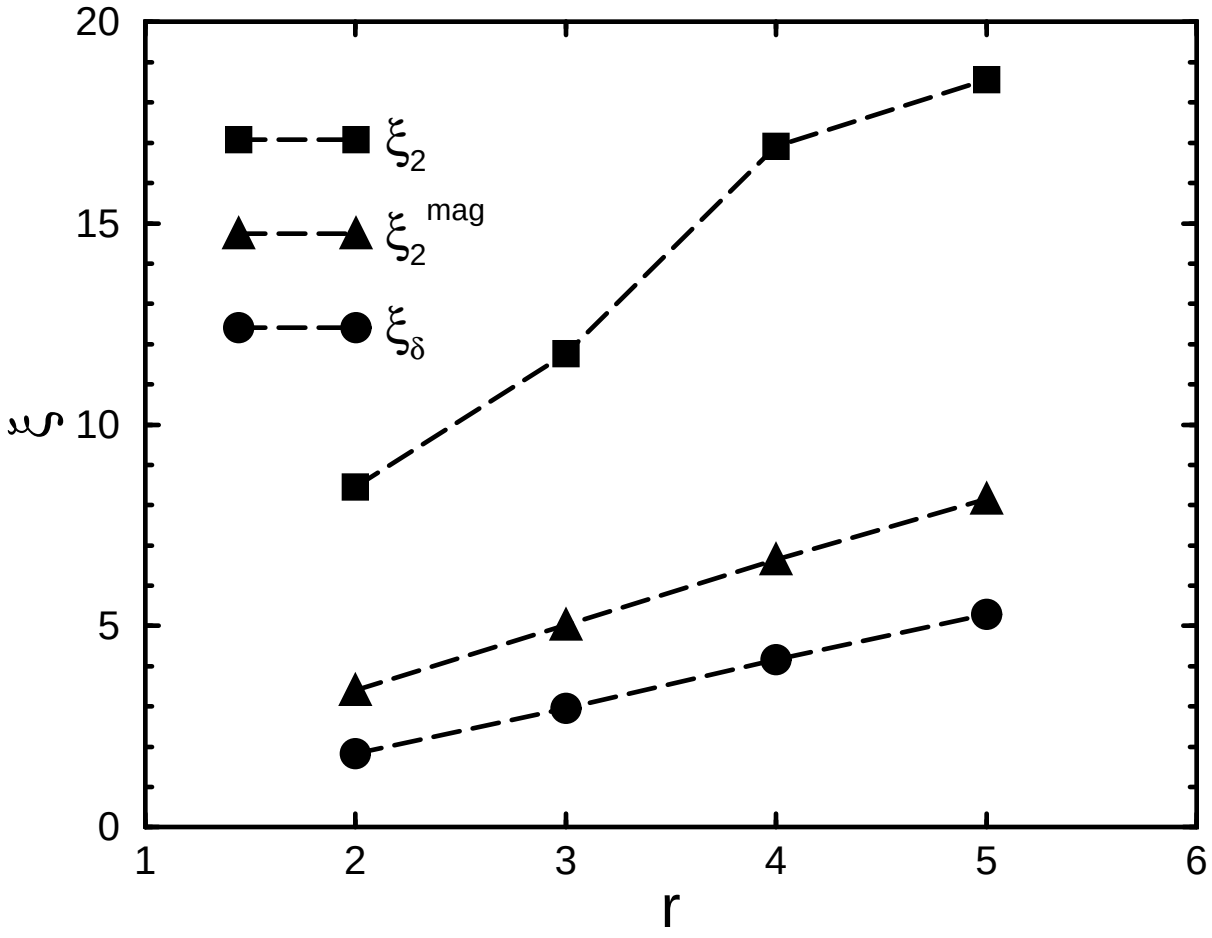

Figure 15. O'Hern et al. Lyapunov Spectral Analysis...